Study of bacterial cellulose synthase by recombinant protein

2017

Sun Shijing

Contents

List of Publications

This thesis is written based on following publications in scientific journals.

1. Imai T, Sun S-j, Horikawa Y, Wada M, Sugiyama J (2014) Functional reconstitution of cellulose synthase in *Escherichia coli*. Biomacromolecules 15:4206-4213
2. Sun S-j, Horikawa Y, Wada M, Sugiyama J, Imai T (2016) Site-directed mutagenesis of bacterial cellulose synthase highlights sulfur-arene interaction as key to catalysis. Carbohydr Res 434:99-106
3. Sun S-j, Imai T, Sugiyama J, Kimura S (2017) CesA protein is included in the terminal complex of *Acetobacter*. (Submitted)

List of Abbreviations

ATR, attenuated total reflection;

BSA, bovine serum albumin;

CBB, coomassie brilliant blue;

c-di-GMP, cyclic-di-guanyl monophosphate;

CID, collision induced dissociation;

CSC, cellulose synthase complex;

DGC, diguanyl cyclase;

DP, degree of polymerization;

EDTA, ethylenediammine-N,N,N',N'-tetraacetic acid;

ESI, electrospray ionization;

FTIR, Fourier transform infrared;

GPC, gel permeation chromatography;

GT, Glycosyltransferase;

IPTG, isopropyl-thio-β-d-galactoside;

LC/MS, liquid chromatography/mass spectrometry;

PAGE, poly-acrylamide gel electrophoresis;

PASC, phosphoric acid swollen cellulose;

PBS, phosphate-buffered saline;

PCR: polymerase chain reaction;

PFA, paraformaldehyde;

PVDF, polyvinylidene difluoride;

RBS, ribosomal binding site;

RT, room temperature;

SDS, sodium dodecyl sulfate;

TBS, tris-buffered saline;

TC, terminal complex;

TCA, trichloroacetic acid;

TIC, total ion chromatogram.

Chapter 1 General introduction

Cellulose is one of the most abundant biological polymers on Earth. It is a high-molecular-weight polysaccharide produced by all plants, algae, protists, some bacteria, and animal tunicates. As cellulose is the main components of plant cell wall in wood and cotton, it has been used for a long time ago. It is also used as an important industrial biopolymer in textiles, paper, construction materials, and so on. Cellulose produced from bacteria is also used widely in medical, electric devices, food and fine chemical industry and so on (Czaja et al. 2006; Klemm et al. 2009). Now due to the technology developing, cellulose could be used in many new areas. For example, cellulose can be a renewable energy source, owing to the production of ethanol by bioprocess of enzymatic saccharification and fermentation (Mizrachi et al. 2012). Another new type utilization of cellulose is nanocellulose, which could be used as car material and maybe the aerospace field (Yano 2013; Isogai 2013). However, there are still a lot of problems for using cellulose. In biofuel production for example, cellulose must be purified from other cell wall components and this process is energetically expensive and environmentally unfriendly. Therefore, it is valuable to research, how to get the pure cellulose, how to increase the cellulose production, and how to improve the utilization of cellulose. For these purposes, study of the biosynthesis of cellulose must be the required basic knowledge.

Cellulose biosynthesis is actually multi-step process. Generally, at first, cellulose synthase, a membrane-bound Glycosyltransferase Family 2 (GT-2) enzyme, catalyzes β1→4-glucan chain polymerization using substrate UDP-glucose. Secondly, cellulose

synthase proteins typically arrange themselves into multimeric cellulose synthase complexes (CSC), which are required for the production of multichain cellulose microfibrils (Sethaphong et al. 2013). CSC is embedded in the lipid bilayer of cell membranes and is a heterosubunit complex of several different protein subunits. Therefore, it has been a difficult protein to analyze, and our biochemical understanding of cellulose biosynthesis remains limited. Despite some progresses on genetic, biochemistry, and structural biology (reviewed by Slabaugh et al 2014; Römling and Galperin 2015; McNamara et al. 2015), we do not know very well how many proteins are involved in synthesizing cellulose, what is the function of each subunit and how these proteins get glucose into cellulose chain and further assemble them into a crystallized microfibril. Thus, this introduction covers the background of structure, biogenesis of cellulose and the in vitro synthesizing of cellulose for understanding the processing of cellulose synthesis.

1.1 Solid state structure of cellulose

As the properties of cellulose directly connect to the structure, the structure has been intensively investigated. It is well known that it exist as crystalline fiber. The biosynthesis cellulose chains are crystallized into a microfibril by hydrogen bonding and van der Waals forces (Nishiyama et al. 2002; 2003). There are mainly four crystallographic polymorphs: I, II, III and IV (Sarko 1978). The polymorph is defined by its unit cell parameters. The structure and morphology of native cellulose will be related to biosynthesis. Therefore, understanding the solid state structure of cellulose is helpful for knowing the mechanism of cellulose biosynthesis.

Cellulose I is the native form except for a few exceptions. Cellulose I consists of extended parallel glucan chains (Preston 1974). In 1937, Meyer et al. suggested unique crystalline lattice for native cellulose by X-ray diffraction patterns (Meyer and Misch 1937). The unit cell was monoclinic with two antiparallel cellobiose units, one at corner and one at the center of the cell. Cell parameter is a=7.9 Å, b= 8.35 Å, c=10.3 Å, γ=96 ° (Wertz et al. 2010).

Cellulose I was investigated by NMR and it was shown that cellulose I has two allomorphs I_α and I_β (Atalla and VanderHart 1984). The crystallographic unit cell for I_α and I_β, determined by electron microdiffraction, is one-chain triclinic (*P1* space group) and two-chain monoclinic unit cell ($P2_1$ space group), respectively (Sugiyama et al. 1991b). The one-chain triclinic structure requires all the chain to be pached parallel. *d* Spacings of 0.60, 0.53 and 0.39 nm respectively are indexed as $(100)_t$, $(010)_t$, $(110)_t$ in the triclinic unit cell and as $(1\,\bar{1}\,0)_m$, $(110)_m$ and $(200)_m$ in monoclinic cell. Native cellulose is classified as either I_α- or I_β-rich types. Most of plants synthesize I_β-rich cellulose while bacteria synthesize I_α-rich cellulose (Hayashi et al. 1997; 1998). I_α phase is metastable and can be converted into thermodynamically stable I_β phase by hydrothermal treatment or annealing (Yamamoto et al. 1989). The conversion of I_α to I_β was detected by Fourier transform infrared (FT-IR) spectroscopy (Sugiyama et al. 1991a). Absorption bands near 3240 and 750 cm^{-1} were assigned to the I_α phase whereas 3270 and 710 cm^{-1} corresponded to the I_β phase.

Cellulose II is mostly prepared from cellulose I by two distinct routes, one is mercerization and the other is regeneration. Only a few organisms naturally synthesize cellulose II (Brown 1996). When cellulose I is treated by strong alkaline conditions, crystallographic form becomes into thermodynamically more stable cellulose II. This

process is called mercerization. And this transformation is irreversible. When cellulose I solubilized or recrystallized it is called regeneration. In 1929, Andress proposed a monoclinic with two antiparallel cellobiose segments for mercerized cellulose. Continuously, other researchers have investigated it and the two cellulose chain lie antiparallel to one another is the most prevalent view (Sarko and Muggli 1974; Kolpak and Blacwell 1976; Stipanovic and Sarko 1976). In 1988, Simon et al. proposed the possibility of parallel cellulose I converted to antiparallel cellulose II.

Cellulose III is derived from cellulose either I or II, and they are called cellulose III_I and III_{II}, respectively. Cellulose III is formed by swelling cellulose I or II with amines or liquid ammonia and subsequently removing the swelling agent anhydrously. In 2001, Wada et al. obtained an improved structure for cellulose III_I by highly crystalline cellulose samples. The cell parameters were: a=4.48 Å, b=7.85 Å, c=10.31 Å, γ=105.1°. In addition, CP (cross polarization)/ MAS (magic angle spinning) ^{13}C-NMR spectra showed the hydroxymethyl group adopts the *gt* conformation. It was suggested that the single chain of cellulose III_I might have some conformational similarities with one of the two chains of cellulose II (Wada et al 2001).

Cellulose IV is classically formed by annealing cellulose III in glycerol and they are called cellulose IV_I, and IV_{II}, depending on whether the starting material is cellulose III_I and III_{II}. Unit cell parameters were proposed as a=8.03 Å, b= 8.13 Å, c=10.34 Å, γ=96° for IV_I, and a=7.99 Å, b= 8.13 Å, c=10.34 Å for IV_{II} (Pérez and Mackie 2001).

All above is about the definition, properties and localizations of different types of crystallographic polymorphs of cellulose. These structures are not only related to the mechanical property of cellulose but also to related to the cellulose synthase. By knowing these structures of cellulose, we can have more understandings of the cellulose

microfibril synthesizing proteins namely CSC and the mechanism of cellulose biogenesis.

1.2 Biogenesis of cellulose

In contrast to the studies of structure, the biogenesis of cellulose starts to be studied late. The first cellulose synthase gene was identified in 1990 from *Acetobacter xylinum* (now renamed for some strains as *Gluconacetobacter*, *Komagataeibacter*, and so on), (Saxena et al. 1990; Wong et al.1990). In the case of this bacterial species, four subunits are proposed to be included in the CSC: GxCesA, GxCesB, GxCesC, and GxCesD (formerly BcsA, BcsB, BcsC, and BcsD). In all of cellulose-synthesizing organisms, CesA (cellulose synthase A) is included as the catalytic subunit. Other auxiliary subunits are also included in CSC. However, many questions remain to be answered as follows: how many proteins are involved in CSC and how these cellulose synthases subunits cooperate and interact with each other, and what is the function of the auxiliary proteins to synthesizing cellulose. Here, we show the advance understanding about CesA and other subunits separately and then move to the CSC, which is an assembly of these proteins.

1.2.1 Cellulose synthase A (CesA)

CesA is a protein to link glucose residues by β1→4-linkage and carrying the glycosyltransferase domain of the GT-2 family in CAZy database. GT-2 family also contains chitin synthases, β1→3-glucan synthase hyaluronan synthase (HAS), alginate synthase (AlgS). Since 1990, CesA genes were identified in a lot of bacterial species: *Gluconacetobactor henssii, Rhizobium leguminosarum, Agrobacterium tumefaciens,*

and *Escherichia coli* (Zogaj et al. 2001; Serra et al. 2013; Römling and Galperin 2015). In plants, *CesA* genes were also identified from *Arabidopsis*, Maize, barley, poplar and so on (Somerville 2006).

In 1995, by hydrophobic cluster analysis of amino acid sequences, Saxena et al. clarified that GT-2 family β-glycosyltransferases have two domains (domains A and B), which include D, D motif and D, QxxRW motif sequences, respectively (Saxena et al. 1995). Domain B was proposed to be important for chain elongation since it was found only in polysaccharide synthases. In 1997, Saxena and Brown analyzed the first two conserved aspartic acid residues by site-directed mutagenesis, and their replacement by another amino acids led to a loss of cellulose synthase activity in *A. xylinum*, suggesting that they are essential for enzyme activity (Saxena and Brown 1997). Other groups also directly showed that these domain A amino acid residues are involved in polysaccharide synthesis (Nagahashi et al. 1995; Dorfmueller et al. 2014).

The role of these motif sequences was studied not only by sequence comparisons and site-directed mutagenesis, but also structural biology. In 2013, Morgan et al. reported the first three-dimensional structure of cellulose synthase A and B from a purple bacterium *Rhodobacter sphaeroides* (Morgan et al. 2013). CesA protein has eight transmembrane (TM) helices. Between TM4 and TM5, the catalytic GT-2 domain is inserted and formed a classical GT-A fold, which contains the N-terminal, four-stranded, parallel β-sheets and forms the binding site for the substrate UDP-glucose. The GT domain includes the famous QxxRW motif also. This motif is located in an interfacial α-helix (IF2) running on the inner surface of the lipid bilayer, and plays an important role for keeping acceptor cellulose molecules in the correct position for the glucosyltransfer. RsCesA contains the C-terminal cytosolic domain termed PilZ, which

is responsible for c-di-GMP binding (Christen et al. 2007; Amikam et al. 2006). In addition to these well-known motifs, the structural model of cellulose synthase indicated other important motifs in CesA, such as QTPH and FFCGS.

In plants, the first cellulose synthase gene was identified by Pear et al. in 1996. They surveyed the cDNA library of cotton in 21 days post anthesis, and discovered the sequence showing a homology to bacteria CesA (Pear et al. 1996). The completion of the *Arabidopsis* genome sequencing project revealed that *Arabidopsis* has 10 CesA genes that encode proteins with 64% average sequence identity to each other (Holland et al. 2000; Richomnd 2000). Maize has at least 12 CesA genes, barley has at least 8, and poplar has at least 7 (Somerville 2006). In *Arabidopsis* three of them are responsible for the cellulose synthesis in primary cell wall formation (AtCesA1, AtCesA3, AtCesA6), while AtCesA4, AtCesA7, AtCesA8 are required for secondary cell wall formation (Somerville 2006). Plants CesA also contains the conserved D, D, D, QxxRW motif (Pear et al. 1996), but also has plant-conserved region (P-CR) and a class specific region (CSR), neither of which was found in bacteria. For the QxxRW motif, QVLRW is more popular in plants CesA while bacteria and tunicate CesA have the sequence of QRxRW (Somerville 2006).

1.2.2 Auxiliary subunits in CSC

In addition to the catalytic subunit CesA, CSC also includes auxiliary subunits for most of species. In the case of *Acetobacter*, cellulose synthase subunits, which are composed into cellulose biosynthesis, involve CesB, CesC, CesD (Saxena et al. 1994), Ccp (cellulose complement protein) (Standal et al. 1994), BglxA (Tonouchi et al. 1997)

and glycoside hydrolase family 8 (GH-8, also known as carboxymethyl cellulase CMCax-or CesZ) (Standal et al. 1994).

CesB with CesA are the minimally required subunits for cellulose-synthesizing activity (Omadjela et al. 2013, Saxena et al. 1994, Wong et al. 1990). *CesB* gene is found in all the bacterial cellulose synthase operons (Römling et al. 2013). The crystallographic structure clearly shows that the C-terminal transmembrane helix anchored in the lipid bilayer. The remained main parts of CesB extend about 60 Å into periplasm. It includes two copies of a repeating unit of carbohydrate-binding domain (CBD) that C-terminary fused to an α/β domain resembling a flavodoxin-like domain (FD). Truncating the N-terminal of CesB revealed that only C-terminal TM anchor and the preceding amphipathic helix required for cellulose-synthesitzing activity (Omadjela et al. 2013).

Although CesA, CesB and c-di-GMP are necessary for robust cellulose-synthesizing activity in vitro, genetic analyses show that CesC subunit is necessary for maximal cellulose synthesis and secretion in vivo (Saxena et al. 1994). However, until now the crystallographic structure of CesC has not been reported. CesC is a large protein. According to sequence analysis, CesC is considered to be separate to two parts. One of the parts is located in the outer membrane. The other N-terminal part in periplasm of cell is a large domain with tetra-tricopeptide (TPR)-like repeats. And this part may be involved in protein and protein interaction (Keisski et al. 2010; Zeytuni et al. 2012). CesC is similar to components of bacteria alginate synthase, AlgE and AlgK protein (Keisski et al. 2010). It is hypothesized that the outer membrane part is similar with AlgE and form a pore in the outer membrane. And the N-terminal part of CesC is similar to AlgK that includes TPR domains. However, we do not yet know whether

CesC directly interact with subunits CesA and CesB, or not (McNamara et al. 2015). As well, it has to be clarified how the periplasmic domain of CesC interacts with the translocating cellulose chain and how cellulose enters the outer membrane channel (Whitney et al. 2011).

CesD is the subunit not essential for cellulose biosynthesis in bacteria but knock out mutant of *CesD* showed that the reduced cellulose production as well as lower crystallinity of the produced cellulose in vivo (Saxena and Brown 2012). The crystal structure of CesD from *Acetobacter xylinum* is the earliest reported cellulose synthase subunit (Hu et al. 2010). It is a barrel-shaped tetramer of dimmers and has four passageways for emerging glucans. However, it has not been demonstrated how the synthesized glucan chains from CesA are transferred to CesD.

Ccp was found colocalized with CesD. This interaction was proved by pull-down experiments and isothermal titration calorimetry (Sunagawa et al. 2013).

BglX is a β-glucosidase. The *bglxa* gene is located downstream of the bacterial cellulose synthesis operon (Tonouchi et al. 1997). The disruption of *bglxa* causes a decrease in cellulose production (Kawano et al. 2002).

GH-8 was identified in all cellulose-producing bacteria. It is a β1→4-glucanase. In 1994, it was reported that GH-8 is required for cellulose production and is a gene colocalized with bacteria cellulose synthase in *Acetobacter xylinum* (Standal et al. 1994). In 1998, Koo et al. also found that a β1→4-endoglucanase plays an essential role for the formation of cellulose microfibril. In 2013, Nakai et al. proved the formation of highly twisted ribbons in a carboxymethyl cellulase gene-disrupted strain. Although the biological purpose of the hydrolytic activity during cellulose synthesis is unknown, it is possible that glucanases are required for the controlled alignment of individual

β1→4-glucan strands to form the cellulose microfibril. Cellulase is not only involved in the cellulose production by bacteria but also by plants namely KORRIGAN (Mazur O and Zimmer J 2011).

Despite less knowledge than the bacterial cellulose synthase, plant cellulose synthase is also supposed to be a heterosubunit complex. Many studies have proposed candidate proteins for the subunits included in CSC, like sucrose synthase (Fujii et al. 2010), cytoskeleton (Green 1962), CesA interacting protein (CSI1/POM1) (Gu et al. 2010), KORRIGAN (KOR) (Nicol et al. 1998;Lei et al. 2014; Vain et al. 2014), COBRA-like protein (Schindelman et al. 2001; Roudier et al. 2005).

As the UDP-glucose is the substrate, sucrose synthases might associate with CSC to provide a local supplement (Fujii et al. 2010). The cytoskeleton also plays important roles in cellulose synthesis. The well known is cortical microtubules (reviewed by Bringmann et al. 2012; Landrein and Hamant 2013; Paradez et al. 2006). The orientation of cortical microtubule alignment was altered in *CesA2* and *CesA6* mutants and isoxaben-treated cells, which are all defective in cellulose synthesis (Chu et al. 2007; Fisher and Cyr et al. 1998; Paredez et al. 2008), suggesting that feedback may exist between CSCs and the cortical microtubule array. POM2/CSI1 is a candidate protein that directly links CSCs to the cortical microtubule array. CSI1 interacted with microtubules in vitro (Li et al.2012; Mei et al. 2012).

The KOR protein, which appears to be expressed in all cells, encodes a membrane-localized β1→4-endoglucanase. Mutations in *kor* gene exhibit reduced cellulose accumulation and changes in pectin composition that presumably reflects responses to the cellulose defect (His et al. 2001; Nicol et al. 1998; Sato et al. 2001). A number of other mutant alleles of the *kor* gene have been found. These include *rsw*2,

which exhibits a temperature-sensitive defect in cellulose accumulation (Lane et al. 2001), as does another allele identified by Sato et al. (2001) and the *irx2* mutation (Szyjanowicz et al. 2004). However, the role of KOR is unknown. Although some researchers got the localization results, no clear evidence for an association with cellulose synthesis has been provided (Brummell et al. 1997; Robert et al. 2005; Zuo et al. 2000). In 2006, live-cell imaging of individual cellulose synthase complexes tagged with yellow fluorescent protein (YFP) has revealed that it is possible to visualize discrete complexes in the plasma membrane (Paredez et al. 2006). Based on the functional evidence, Somerville (2006) hypothesized that KOR is associated with the CesA complex. In 2014, Vain et al. used live-cell imaging with split ubiquitin and fluorescence complementation assays and suggested that KOR is indeed an integral component of CSC in *Arabidopsis* membranes.

The *cobra* gene encodes a glycolsphatidyl inositol (GPI) -anchored plant-specific protein of unknown function (Schindelman et al. 2001). Null COBRA mutants are extremely deficient in cellulose and are strongly dwarfed. It has been suggested that COBRA protein specifically controls highly anisotropic expansion through its involvement in cellulose microfiberil orientation (Roudier et al. 2005).

Despite extensive studies on such many auxiliary subunits, there are many issues to be addressed for understanding how these subunits are involved in cellulose biosynthesis.

1.2.3 Cellulose synthase complex

Cellulose synthase complex is proposed in 1958 by Roelofsen, who suggested that the native cellulose might be synthesized and crystallized by the action of a large

enzyme complex (Roelofsen 1958). The first cellulose synthase complex was visualized in the plasma membrane of unicellular green alga *Oocystis apiculata* by freeze replica technique of electron microscope (Brown and Motezinos 1976). It shows an orienting and linear row of 12nm-particles located in the protoplasmic fracture face (PF) of out membrane. As this complex is found at the end of synthesizing microfibril, it is called terminal complex (TC). The variable morphologies of TCs in the organisms have been widely investigated and summarized by Brown (Brown 1996). The basic patterns are linear and rosette. TC in bacteria is the linear type. In higher plants, rosette type TCs are found, and it was shown in 1999 that plant rosette TC includes CesA protein by SDS-FRL (freeze replica labeling) (Kimura et al 1999). For the linear TC of *Acetobacter*, CesB protein was demonstrated to be included (Kimura et al 2001), as well as CesD, and ccp (Sunagawa et al. 2013).

Although we have known that some subunits are included in CSC, we do not yet know relative localization of each subunit. According to the results reported, some schematic diagrams about the position of these subunits in CSC have been proposed in different species.

In *Acetobacter*, a model of cellulose-synthesizing organism has been searched a lot on the gene and subunits. After getting the sequencing the genes of cellulose synthase from *Acetobacter*, Brown proposed the organization of the major subunits of cellulose synthase namly CesAB, CesC, CesD (Brown 1996). Schematic diagram shows that CesAB located in the inner membrane. CesC forms the major channel for export of the cellulose from the inner membrane to the cell surface and CesD located in the deep of the channel with binding to the CesAB and CesC (Figure 1.1A). At the same time, he

also proposed another diagram according to the results of CesD mutant produced cellulose II (Brown 1996).

In the model in 2010, CesD is located in the outer membrane (Endler 2010). The next year, Iyer et al. proposed CesD is in the periplasm by biochemical evidences. The model showed the pore in CesD allows extrusion of one microfibril of average diameter 3-6 nm (Figure 1.1B) (Iyer et al. 2011). In 2015, McNamara et al. proposed that CesAB complex form the catalytic core at the inner membrane. And maybe interact with the periplasmic domain of CesC (Figure 1.1C). CesZ may cleave the translocating glucan in the periplasm, while the role of CesD is unclear (McNamara et al. 2015).

The same year, Römling and Galperin proposed several models for the CSC in bacteria. For *Acetobacter*, it is almost same with McNamara shown (Figure 1.1D). They also proposed a model for *E.coli*. Differently from *Acetobacter*, *E.coli* has CesE (Cellulose synthase cytoplasmic subunit and binds c-di-GMP), CesF (Membrane-anchored subnit), CesG (Contains 4 TM segments and a peiplasmic AlKP domain) proteins but not CesD, in addition to CesAB, CesC and CesZ proteins (Figure 1.1E) (Römling and Galperin 2015). In 2016, the structural model for *Gh*CesAB complex was proposed from single particle analysis of electron microscopy. They proposed the model for CesA, B, C, D complex in relation to cellulose polymerization and secretion (Du et al. 2016). The model includes those four subunits of CesAB complexes are embedded in the inner membrane, each of which synthesizes one cellulose chain. Then the four glucan chains from four CesAB complexes are bundled by CesD octamer. Finally the cellulose chains are extruded out of the cell through CesC located in the outer membrane (Figure 1.1F) (Du et al. 2016).

About higher plants, along the time some schematic models also were proposed. In 2006, Somerville showed a schematic model of higher plants cellulose synthesis. Cellulose synthesis takes place in the plasma membrane. The cellulose synthase complex of rosette is thought to contain 36 CesA proteins, only a subset of which is illustrated. That three types of CesA proteins are required to form a functional complex. And this suggested that different types of CesA proteins perform specific functions, such as interacting with the cortical microtubules. KOR may participate in cellulose synthesis (Somerville 2006). In 2010, Guerriero et al. also proposed that each of the subunits in the rosette includes three different isoforms to form 8-nm subunit, and hexagonal packing of them forms the 25-nm rosette. And the possible roles of KOR for cellulose synthesizing were also showed (Guerriero et al. 2010). In 2014, Heather et al. shows that the intracellular, membrane and extracellular environment may affect velocity of CSC, which includes cortical microtubules and sucrose synthase in intracellular environment, shingolipids and sterols in the plasma membrane, KOR and CSI1 interacting with CSC and COBRA and CTL1 in extracellular proteins.

Despite such intensive studies above, we do not completely figure out the CSC regardardless of the species. It is then still necessary to establish a method to visualize and analyze these components.

1.3 In vitro synthesis of cellulose

For knowing the mechanism of cellulose synthesis, many attempts to synthesize cellulose have been made in vitro with cell-free system. Researchers have tried to synthesize cellulose from prokaryotic to eukaryotic different sources since 1950s.

A lot of researchers have investigated *Acetobacter xylinum*. Delmer et al. reported that a membrane potential for cellulose synthesis in intact cells of *Acetobacter xylinum* is required (Delmer et al.1980). Aloni et al. achieved high rates of in vitro synthesis of cellulose by membranes in the present of polyethylene glycol (PEG) and guanosine triphosphate (GTP) (Aloni et al. 1982). Bureau et al. synthesized cellulose II by isolating discountinuous sucrose density from an inner membrane fraction of *Acetobacter xylinum* (ATCC 53582) in vitro (Bureau et al. 1987). Lin et al. synthesised fibrils in vitro by a digitonin-solubilised cellulose synthase from *Acetobacter xylinum* (Lin et al. 1988).

In vitro synthesizing cellulose by plant is difficult because high background of callose-synthesizing activity is found at some time. Nevertheless, Kudlicka et al. synthesized β-glucan with Mops buffer and sucrose by using two digitonin extraction protocols of plasma membrane of cotton fiber. The extract by lower concentration of digitonin synthesized cellulose I while higher concentration of detergent gave cellulose II production. However, both of these two conditions synthesized callose (Kudlicka et al. 1995). Callose and cellulose synthase activities were first completely separated by native gel electrophoresis in non-denaturing conditions (Kudlicka et al. 1997), and visualized a rosette-TC-like structure in the detergent extract. In 2002, Lai et al. isolated cellulose-synthesizing activity in vitro from *Rubus fruticosus* (blackberry). Colombani et al. in vitro synthesis of β1→3-D-glucan (callose) and cellulose by detergent extracts of membranes from cell suspension cultures of hybrid aspen (Colombani et al. 2004).

Our lab also reinvestigated the synthesis of cellulose in vitro with a well-known cellulose-producing bacterium, *Gluconacetobacter xylinus* (fromly *Acetobacter xylinum*) (Hashimoto et al. 2011). It was the first time to check the cellulose-synthesizing activity

for the alkylamaltoside extract from the cell membrane in comparison with the previously used detergents, digitonin and Triton X-100. However, activity comparable to that previously reported is obtained, while the synthesized cellulose is crystallized into a non-native polymorph of cellulose (cellulose II) as well as the previous studies.

Despite the numerous studies available on a large number of pro- and eukaryotic model systems, revealing the mechanism of cellulose synthesis and translocation has been hampered by difficulties in reconstituting functional CesAs in a purified system. To 2013, cellulose biosynthetic activities have only been recovered from detergent extracts of native membranes (Aloni et al. 1982; Lai et al. 2002; Guerriero et al. 2010)

In 2013 however, Omadjela et al. showed cellulose-synthesizing activity in vitro for recombinant cellulose synthase of *Rhodobacter* RsCesAB complex (Omadjela et al. 2013). The purified complex efficiently synthesizes amorphous, high-molecular-weight (HMW) cellulose on incubation with UDP-glucose and c-di-GMP, both in a detergent-solubilized state and after reconstitution into proteoliposomes (PLs).

Excitingly not only successful reconstituted bacteria cellulose synthase, recently, Purushotham et al. expressed one isoform of poplar *CesA* (*CesA8*) to produce cellulose, indicating that a single heterologously expressed plant cellulose synthase isoform is sufficient for cellulose microfibril formation in vitro (Purushotham et al. 2016).

However, both these two successful in vitro reconstitute of bacteria and plant cellulose synthase，radioactive substrate is required for quantify the production. Even it is a rapid and reliable method, specialized facilities are needed and it is not easy to handle out.

1.4 Objectives of the thesis

As cellulose is used so common and it is an environment friendly nature polymer, efficient utilization has been required. However, the process of cellulose biosynthesis is still not clear very well, because the cellulose synthase is a membrane-integrated protein. The purification of cellulose synthase is difficult. Especially in higher plants, the subunit organization in the CSC is not clear despite extensive works given even more complicated system than bacterial. The product of in vitro synthesized cellulose by plants is a much smaller amount than bacteria and also containing higher level callose which bacterial model does not produce. Then in order to make a function analysis of cellulose biosynthesis, bacteria cellulose synthase is still a good model.

The major purpose of this study is to make a functional reconstitution of bacteria cellulose synthase for function analysis of cellulose synthase. *A. xylinum* is a classic model for cellulose biosynthesis research and *E.coli* is a very common tool for studying protein. In chapter 2, cellulose synthase of *G. xylinus* was expressed in *E.coli* to have cellulose-synthesizing activity in *E.coli*. In chapter 3, site-directed mutagenesis was conducted by using cellulose-synthesizing *E.coli* prepared in chapter 2 for studying the mechanism of well-conserved amino acid residues in cellulose synthase. In chapter 4, immunolabeling microscopy method was used for figuring out the subunits in the TC of *Acetobacter*, which is very important to bundle the cellulose chains into microfibril.

FIGURE CAPTIONS

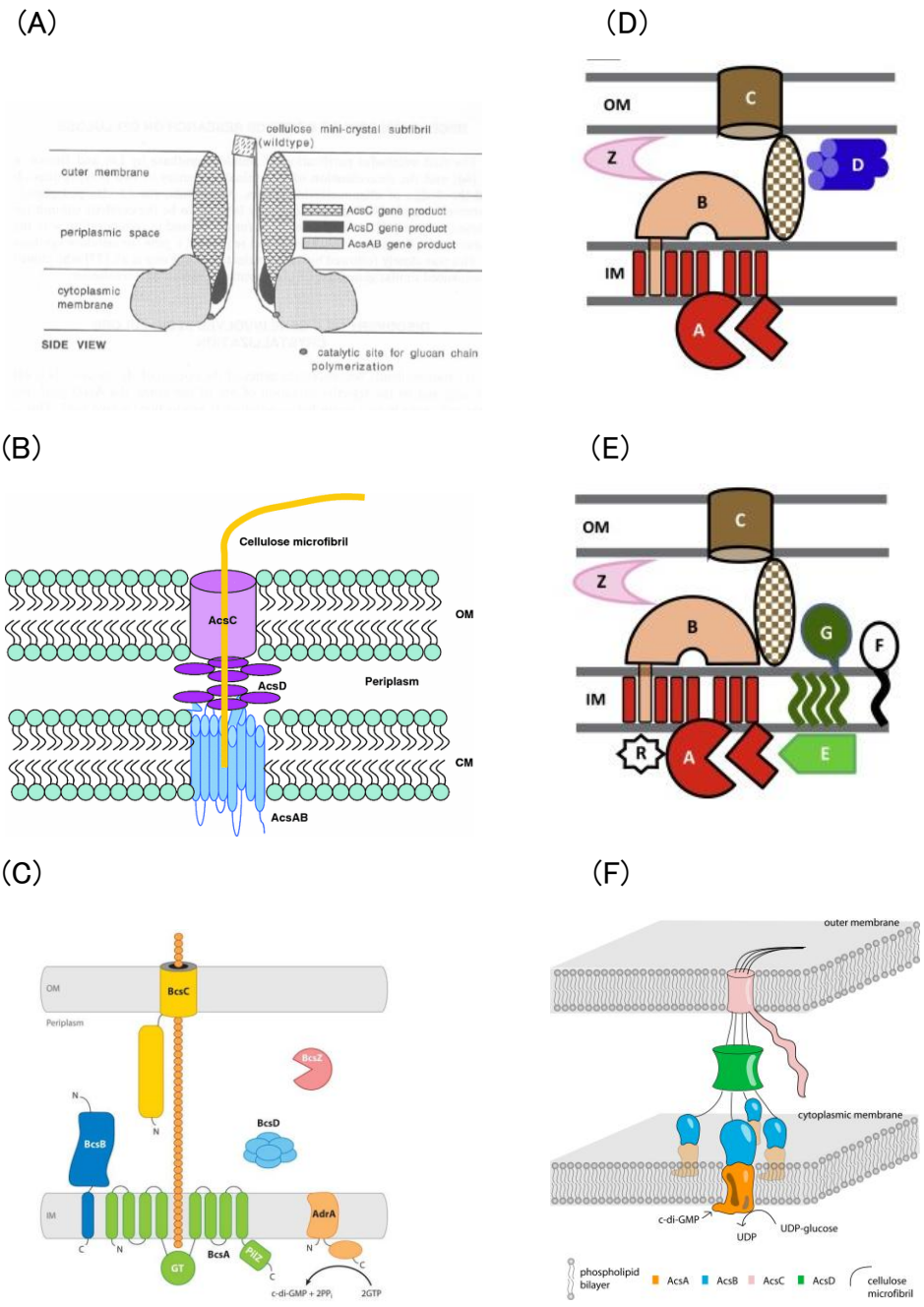

Figure 1. 1 Organization of the cellulose synthase complexes. (**A**) (Brown 1996) (**B**) Model for cellulose extrusion (Iyer et al. 2011) (**C**) The bacterial cellulose synthase (Bcs) contains multiple subunits at the cell envelope. (McNamara et al. 2015) (**D-E**) Proposed organization of the bacteria cellulose synthase complexes from (**D**) *Komagataeibacter xylinus* and (**E**) *Escherichia coli* (Römling and Galperin 2015) (**F**) Schematic representation of proposed cellulose polymerization and secretion complex in *G. hansenii* (Du et al. 2016)

Chapter 2 Functional reconstitution of cellulose synthase in *Escherichia coli* -- CESEC: a system to explore cellulose synthase

2.1 Introduction

Cellulose biosynthesis is a process by which glucose is polymerized by β1→4 linkage, and bunches of β1→4-glucan chains are simultaneously bundled into fibers called microfibrils, in which all chains are oriented in the same direction and are crystallized into the specific crystallographic form of cellulose I (Koyama et al. 1997). This complex process is facilitated by cellulose synthase, which exists as a hetero-subunit protein complex in the cell membrane (Delmer 1999; Someville 2006). The first cellulose synthase gene was identified in a cellulose-producing bacterium *Gluconacetobacter xylinus* (formerly *Acetobacter xylinum*) in 1990 (Saxena 1990). In this bacterium, four genes are clustered in one operon (Wong et al. 1990; Saxena et al. 1994), namely, *gxcesA*, *gxcesB, gxcesC,* and *gxcesD* (formerly *bcsA*, *bcsB, bcsC,* and *bcsD*). GxCesA protein is a GT-2 glycosyltransferase containing transmembrane helices and the catalytic subunit of cellulose synthase. The gene of *cesA* is found in all living cellulose-producing organisms, whereas the other genes are specific to bacteria cellulose synthase. In the case of bacteria, the CesA and CesB proteins represent the minimum subunit requirements for cellulose synthesis (Wong et al. 1990; Omadjela et

al. 2013), and it was recently shown that the auxiliary subunit of CesB interacts with the CesA protein via its C-terminal transmembrane helix (Omadjela et al. 2013). In addition to CesA and CesB, c-di-GMP (cyclic-di-GMP) is required to activate bacterial cellulose synthase (Omadjela et al. 2013; Ross et al. 1987). Recently, X-ray crystallographic analyses were reported for this complex of the bacterium *Rhodobacter sphaeroides* (Morgan et al. 2013; 2014), and these structural models shed some light on the mechanism of cellulose biosynthesis. While some progress has been made in terms of such structural analyses, the paucity of functional analyses is striking, with only a few such studies (Omadjela et al. 2013; Saxena and Brown 1997; Peng et al. 2002; Nobles and Brown, 1997; Su et al. 2011) being published in more than 20 years since the first cellulose synthase gene was identified.

It has been reported in several studies (No Reference Selected) that cyanobacteria with the *gxcesA* and *gxcesB* genes introduced into their genomic DNA can produce cellulose (Nobles and Brown, 1997; Su et al. 2011). In such studies, however, the genes of interest are inserted into the genomic DNA by the relatively laborious procedure of DNA recombination, and functional analyses of such systems demand efficient techniques. Toward establishing an easier experimental system to assess enzymatic activity of recombinant cellulose synthase, an *Escherichia coli* transformant containing conventional plasmid DNA encoding CesA and CesB of *G. xylinus* was prepared.

2.2 Materials and Methods

2.2.1 Plasmid DNA and *E. coli* preparation

The cellulose synthase genes *gxcesA* and g*xcesB* were amplified from *G. xylinus* JCM9730 (provided by the RIKEN Bio Resource Center, Wako, Japan), which is

equivalent to the BPR2001 strain (Nakai et al. 1998). The design of the primers used to amplify the genes was based on the deposited gene sequence (GenBank Accession Number AB010645). A full description of the expression vector construction will be described elsewhere. Briefly, the *gxcesA* gene was amplified by PCR from upstream of the ATG start codon (-13) to the stop codon of *bcsA*. This sequence was inserted by ligation between the *Eco*RI and *Kpn*I sites of the pQE-80L plasmid (Qiagen Inc.), yielding the CesA-expressing vector. The upstream sequence of *gxcesA* (5′-GGACGAGCTATTG-3′) was assumed to include the putative ribosomal binding site (RBS). The vector to co-express CesA and CesB was prepared by ligation of the *gxcesAB* gene, which was also amplified from upstream of *bcsA* (-13) to the stop codon of the *gxcesB* gene in the form of an operon, at the *Eco*RI and *Kpn*I sites of the pQE-80L plasmid. The two vectors encoding CesA and CesAB thus do not include the RBS of the pQE vector, but rather contain the original RBS of *G. xylinus*. These vectors furthermore contain a scar sequence (5′-GATTATATAA-3′ for the sense strand), which is carried over from the pGEM-T easy plasmid (Promega Inc.) used for subcloning, between the *Eco*RI site of pQE plasmid and the amplified DNA sequence.

The diguanyl cyclase (DGC) protein in this study was encoded by the TM1788 gene of *T. maritima* MSB8 (GenBank Accession Number: NC_000853), which was supplied by the National Bio Resource Center (NBRC) at the National Institute for Technology and Evaluation (Kisarazu, Chiba, Japan). This DGC protein has been reported to have substantial activity for the *in vitro* synthesis of c-di-GMP (Rao et al. 2009). The *dgc* gene was inserted into the pBAD-202 plasmid using the TOPO-cloning strategy (Life Technologies Inc.) to yield a vector encoding thioredoxin-fused DGC. This vector was digested with *Mlu*I and *Sac*I to generate the DNA fragment from the promoter site to the

end of *dgc* gene. This fragment was then inserted between the *Mlu*I and *Sac*I sites of the pBAD33 plasmid (Guzman et al. 1995) (supplied by the National Institute of Genetics (NIG), Mishima, Japan) to produce a DGC-expressing vector. The pBAD33 plasmid contains a p15A origin of replication, which is compatible with the ColE1 origin of replication of the pQE vector. This compatibility allows for the pBAD33 and pQE vectors carrying cellulose synthase genes to be maintained in a single *E. coli* cell. Transformants containing both plasmids can be selected for by treatment of cultures with ampicillin and chloramphenicol.

Unless otherwise stated, the *E. coli* strain used in this study was the XL1-Blue strain. A mutant *E. coli* strain (JW5665 in the Keio collection (Baba et al. 2006)) lacking most part of *bcsA* gene (bacterial *cesA*) was also used in this study, and was supplied by the National Institute of Genetics, Mishima, Japan (NBRP-*E. coli* at NIG). The constructed DNA plasmids were introduced into *E. coli* JW5665 cells after the kanamycin-resistant gene cassette inserted in the target gene (*bcsA*) was removed from its genomic DNA with the aid of a pFT-A vector as previously described (Martinez-Morales et al. 1999).

2.2.2 Recombinant protein expression

E. coli transformants were cultured in 2 × YT medium containing 100 μg/mL ampicillin and 50 μg/mL chloramphenicol, as well as 25 μg/mL tetracycline in the case of XL1-Blue cells. The expression of cellulose synthase and DGC was induced by 0.4 mM isopropyl-thio-β-D-galactoside (IPTG) and 0.2% L-arabinose, respectively, and protein expression was induced at a cell density of OD_{600} 0.5-0.7. Cells were further cultured at 28°C for 6-7 h, after which the cells and synthesized cellulose were harvested by centrifugation at 5,000-8,000 × *g* for 10 min.

2.2.3 SDS-PAGE analysis

After centrifugation, cells were resuspended (10 mM Tris-HCl (pH 8.0), 2 mM EDTA, 0.02% NaN_3) and treated with 0.5% SDS sample buffer (50 mM Tris-HCl (pH 6.5), 10% glycerol, 0.5% SDS, 1% β-mercaptoethanol, and a small amount of bromophenol blue in final) at 65°C to obtain the whole cell sample for SDS-PAGE analysis. In non-reducing condition, β-mercaptoethanol was not included in the sample.

A portion of the resuspended cells was subjected to alkaline fractionation (Ito and Akiyama 1991) for the separation of the membrane-integrated proteins from other proteins (soluble proteins and inclusion bodies). Briefly, the resuspended cells were lysed with 0.2 mg/mL lysozyme and three freezing-thaw cycles, after which they were solubilized in 0.1 N NaOH on ice. The resulting cell lysate was subjected to centrifugation at 100,000 × *g* for 30 min at 4°C for separating the membrane-integrated proteins (pellet) from the soluble proteins and misfolded proteins in the form of inclusion bodies (supernatant). The pellet was treated with 5% trichloroacetic acid (TCA) while the supernatant was mixed with 10% volume TCA for the precipitation of proteins. The resulting precipitate was washed with cold acetone, subjected to centrifugation, at 5,000 × *g* for 5 min and air-dried. The final precipitate was dissolved in 10 mM Tris-HCl (pH 8.0), 1% SDS, 2 mM EDTA, and 0.02% NaN_3 by incubation at 37°C.

The whole cell samples and the alkaline fractionated samples were subjected to SDS-PAGE using precast 5/20% gradient polyacrylamide gel (SuperSep Ace, Wako Pure Chemical Industries Ltd., Japan). The gels were analyzed by staining with CBB R-250 (Wako Pure Chemical Industries Ltd., Japan) and western blotting using the

previously described primary antibodies against CesA and CesB protein (Hashimoto et al. 2011). Alkaline phosphatase-conjugated anti rabbit IgG (Promega Inc.) secondary antibody and chromogenic substrates (NBT/BCIP, Promega Inc.) were used to visualize protein bands in western blotting.

2.2.4 LC/MS analysis

Cell culture (1 mL) was centrifuged for the extraction of c-di-GMP from the *E. coli* cells, as per a previously described protocol (Thormann et al. 2006). Briefly, the cells were treated with 1% PFA (paraformaldehyde) on ice for 15 min and resuspended in water. After heating at 100°C for 10 min, ethanol was added (70% final concentration) and the cells were centrifuged at 20,000 × *g*. The supernatant was recovered, evaporated, and dissolved in water. A sample of the reconstituted supernatant corresponding to 0.2 µL culture was injected into a LCMS-IT-TOF (Shimadzu Co., Japan) mass spectrometer with an ESI probe. The sample was analyzed in reverse-phase mode using an Inertsil ODS-3 column (φ = 3 µm, 2.1 mm × 50 mm; GL Sciences Inc., Japan) and a flow rate of 0.2 mL/min with the following gradient: 0% B for 0-5 min; 90% B linearly to 20 min; 90% B for 20-30 min; 0% B for 30-40 min (A: 20 mM ammonium formate in water; B: 0.1% formic acid in acetonitrile). The positive ion of *m*/*z* 691 was identified as c-di-GMP given that the daughter ions detected by CID (collision-induced dissociation) were typically observed at *m*/*z* 540 and 248.

2.2.5 Quantification of the synthesized cellulose

The amount of cellulose present in the culture medium was quantified using the anthrone-sulphuric acid method as described previously (Updegraff 1969). Briefly, a

mixture of glacial acetic acid and concentrated nitric acid (AN-reagent, volume ratio of 8:1) was added to the cell pellet, which was then heated at 100°C for 30 min. After washing once by centrifugation at 2,300 × *g* for 10 min, 1 mL 66% (v/v) H_2SO_4 was added to the pellet, which was then incubated for a further 1-2 h at room temperature. The resulting solution (50 µL) was mixed with water (450 µL) and then 1 mL anthrone reagent (0.2% [w/v] anthrone in concentrated H_2SO_4) was added. After heating at 100°C for 15 min, the absorbance of the solution at 625 nm was measured and, based on the absorbance of a standard cellulose sample (PASC; phosphoric acid swollen cellulose prepared by a previously reported protocol (Stahlberg et al. 1993)), the cellulose content of the solution was calculated.

2.2.6 Microscopic observations of cellulose-synthesising *E. coli*

Cellulose-synthesizing *E. coli* cells were directly observed by fluorescence microscopy and electron microscopy. For fluorescence microscopy, 1 mL *E. coli* culture was subjected to centrifugation, after which the resulting cell pellet was resuspended in 1 mL PFA (4% in PBS) for 1 h on ice. The fixed cells were centrifuged again to remove the PFA solution and were then resuspended in 1 mL PBS. The resulting suspension (10 µL) was placed onto a glass slide treated with 0.1% poly-L-lysine or glow discharge. Calcofluor white stain (10 µL, Fluka, 18909) and 10% KOH solution (10 µL) were sequentially added to the sample on the glass slide. A cover slip was then placed over the stained sample, and fluorescence microscopy images were acquired using an Axioplan epifluorescence microscope with a mercury lamp and the filter set 01 (BP365/12, FT395, LP397; Carl Zeiss Microscopy LLC.). The images were recorded using an Axiocam colour CCD camera (Carl Zeiss Microscopy LLC.).

For electron microscopy, culture medium containing cells and synthesized cellulose was directly deposited on glow-discharged, carbon-coated copper mesh. Before drying the sample, the mesh for negative staining was immediately stained twice with 2% uranyl acetate. For shadowing, the mesh was washed with water and an alloy of Pt/Pd was cast on it by resistance-heating with a vacuum evaporator (AUTO306, Edward Inc.). All of the prepared samples were observed with a JEM-2000EXII electron microscope (JEOL Co. Ltd., Japan) operated at 100 kV accelerating voltage and images were recorded with a CCD camera (MegaView G2; Olympus Soft Imaging Solutions GmbH).

2.2.7 Digestion of the product by cellulase

Culture medium containing cells and synthesized cellulose were deposited on carbon-coated mesh without any staining. The prepared mesh was washed with TBS and water, and then dried. The cellulose sample was treated with a 100-μL droplet of cellulase solution (Celluclast 1.5L, Novozymes) in 50 mM MES-NaOH (pH 5.6), after which the mesh was incubated at 45-50°C for 1 h. The sample was then immediately stained with 2% uranyl acetate for electron microscopy. Electron microscopy was carried out as described above using a JEM-2000EXII with a CCD camera.

2.2.8 Structural analysis of synthesized cellulose

Cellulose present in the centrifuged culture medium was isolated as described in previous studies by either AN-treatment (Updegraff 1969; Okuda et al. 1993) or SDS/NaOH treatment (Hashimoto et al. 2011; Bureau and Brown 1987). The former method is the same procedure carried out for the quantification of cellulose as described

above (treatment with AN-reagent at 100°C for 30 min). In the latter protocol, the pellet resulting from centrifugation was treated with 2% SDS at 100°C for 1 h and with 0.5% NaOH at 100°C for 1 h. After repeated washes by centrifugation, the isolated cellulose was analyzed by FTIR spectroscopy, X-ray diffraction, electron microscopy, and electron diffraction. For electron microscopy, the cellulose suspension was deposited on thin carbon-coated copper mesh and stained twice with 2% uranyl acetate. After drying, the mesh was observed using a JEM-2000EXII electron microscope as described above. For electron diffraction, a cellulose sample was deposited on carbon-coated copper mesh without any staining. A JEM-2000EXII electron microscope was operated at 100 kV with a 20 µm condenser lens aperture and the first condenser lens fully excited in order to create a probe as small as 100 nm. Electron diffraction diagrams were obtained with this probe and recorded on photographic emulsion film (MEM film, Mitsubishi paper milling Co. Ltd., Japan). The *d*-spacings of each diffraction ring were measured by calibration with 111 diffraction of gold (d = 0.2355 nm).

FTIR spectra were acquired in ATR mode with the cellulose sample dried on the single bound diamond probe of the ATR attachment. The measurements were carried out using a Spectrum One or Frontier spectrometer (Perkin Elmer Inc.) with 4 cm^{-1} resolution and 16 integrations. For X-ray diffraction, the cellulose sample was lyophilized and pressed into tablets. X-ray diffraction diagrams were obtained using a vacuum camera mounted on a rotating anode X-ray generator (Rigaku RU-200BH). Ni-filtered Cu-Kα radiation (λ= 0.15418 nm) generated at 50 kV and 100 mA was collimated with a 0.3 mm-diameter pinhole and recorded on imaging plates (BAS-IP SR 127, Fujifilm Corp.). The crystallite size was estimated from the width at half-maximum diffraction based on the Scherrer equation with K = 0.9.

The molecular weight of cellulose was estimated by gel permeation chromatography (GPC) after tricarbanilation of cellulose. The cellulose washed by SDS/NaOH was derivatized to tricarbanilation by employing anhydrous pyridine and phenyl isocyanate, following products obtained were soaked in tetrahydrofuran. GPC analysis was performed at 40 °C on a Shodex GPC-101 highspeed liquid chromatography system equipped with a guard column (Shodex GPC KF-G, Showa Denko KK., Kanagawa, Japan), two 30 cm mixed columns (Shodex GPC KF-806L, Showa Denko KK., Kanagawa, Japan), and UV detector. The calibration curve was prepared using polystyrene standards (Showa Denko K. K., Tokyo, Japan) as first-order approximation between logarithmic molecular weight and retention time. The molecular weight value was calculated using the GPC software, and the degree of polymerization (DP) was obtained by dividing by 519, the molecular weight of the cellulose tricarbanilate monomer.

2.3 Results and Discussion

2.3.1 Reconstitution of cellulose sythase A and B in *E. coli*

The *E. coli* XL1-Blue cells harbouring these vectors were cultured in conventional medium without any supplements like glucose. The correct expression of the GxCesA and GxCesB proteins was confirmed by SDS-PAGE. Both CesA and CesB were shown to be localized in cell membrane of *E. coli* transformant (Figure 2.1A) as well as *G. xylinus* (Figure 2.1B), and CesB expressed by the *E. coli* was shown to contain a disulfide bond as well as *G. xylinus*, as indicated by previous studies (Figure 2.1C, note the different position of the band in reducing and non-reducing condition) (Morgan et al. 2013; Lin and Brown 1988). Despite the correct expression of cellulose synthase by *E.*

coli, the expression of cellulose synthase alone did not result in significant cellulose production. The *E. coli* transformant was, however, found to produce cellulose when DGC (diguanyl cyclase or c-di-GMP synthase) was co-expressed with CesA and CesB. In our system, the expression of cellulose synthase and DGC is separately driven by IPTG and L-arabinose inducers, respectively. The expression of DGC was confirmed by CBB (Coomasie Brilliant Blue) staining of the SDS-PAGE gel (Figure 2.1D) and c-di-GMP was identified in the extract of DGC-expressing *E. coli* cells by LC/MS analysis (Figure 2.2A): 9 pmol c-di-GMP was detected in the extract from 1 μL culture in a typical experiment. Significant cellulose production was observed only when DGC was expressed together with cellulose synthase (Figure 2.2B), providing supportive evidence for the role of c-di-GMP as the activator of cellulose synthase. It was further shown (Figure 2.2B) that CesA alone cannot produce cellulose even when co-expressed with DGC, confirming that, as shown previously (Wong et al. 1990; Omadjela et al. 2013), CesA and CesB represent the minimum subunit requirements for cellulose synthesis.

Cellulose synthesis by endogenous enzyme activity in *E. coli* as reported for several strains (Monteiro et al. 2009) was not ruled out in this study, since slight cellulose production was observed in negative conditions (Figure 2.2B). However, significantly higher levels of cellulose production by *E. coli* expressing CesA, CesB, and DGC confirms that most of the cellulose analyzed in this study was synthesized by recombinant cellulose synthase. Like the XL1-Blue strain, the *cesA*-deficient mutant strain of *E. coli* (JW5665 in Keio collection) only exhibited significant cellulose production when cellulose synthase and DGC were co-expressed (Figure 2.2B). These

findings underlie that the *E. coli* transformant cells used in this study are a suitable model for analyzing recombinant cellulose synthase.

2.3.2 Microscope observation of reconstituted cellulose synthase products

At the end of the culturing time, the culture medium of *E. coli* expressing cellulose synthase and DGC showed weak but significant viscosity, and the cell pellet after centrifugation was more difficult to resuspend in the buffer than usual, indicating that cellulose was secreted outside by the cells. Fluorescence microscopic observation of the culture medium revealed the presence of cocoon-like, calcofluor white-stained structures around the *E. coli* cells (Figure 2.3A). Direct observation of cultured cells by electron microscopy consistently revealed fiber structures around the *E. coli* cells (Figure 2.3B-D). These fibers were relatively straight, and measured $\leq$ 2 nm in width—clearly less than bacterial flagella, when measured by electron microscopy (Figure 2.3C). The thickness of these fiber structures was too small to estimate by metal-cast shadowing on carbon film (Figure 2.3D), as far as we tried. The cocoon-like structures and fine fibers were specifically observed when CesA, CesB, and DGC were expressed together, and the fibrous structures were removed by cellulase treatment in a concentration-dependent manner, while neither blank buffer nor lysozyme treatment removed the structures (Figure 2.4). Given the specific appearance of this fiber structure only when expressing cellulose synthase and DGC, it is strongly supported that the fine fiber observed outside the cell is cellulose.

The culture medium of *E. coli* expressing cellulose synthase and DGC was centrifuged and treated according to one of two protocols that has been used to isolate cellulose: treatment with a mixture of acetic acid and nitric acid (hereafter called as

AN-reagent) (Updegraff 1969; Okuda et al. 1993), or treatment with SDS and NaOH (merged). Preliminary GPC analysis of the product washed by SDS/NaOH showed the existence of high molecular weight fraction around 700 of *DP* in weight-averaged. The residue resulting from washing according to either protocol was shown to be cellulose II crystal, a non-native crystallographic form of cellulose, by FTIR spectroscopy (Figure 2.5A). X-ray diffraction analysis of the sample washed with SDS and NaOH revealed the typical profile of cellulose II (Figure 2.5B), and the size of the crystallite was estimated as 8 nm based on the width of 110 diffraction. Electron microscopy of negatively stained samples after washing according to either protocol showed that the washed products are globular aggregations of around 10 nm, and these globules are tied in a row (Figure 2.5C and 2.5D). This aggregation was shown to give the electron diffraction pattern of cellulose II (inset in Figure 2.5C and 2.5D). Given that the crystallite size estimated from X-ray diffraction matches with the size of globule observed by electron microscopy, the globule observed after washing may be a single crystallite of cellulose II.

2.3.3 Structural characterization of reconstituted cellulose synthase products

Notably, the fibrous structures, as shown in Figure 2.3C and 2.3D, were never observed after chemical treatment, indicating that the fibers were converted to globular aggregations of cellulose II by the chemical treatment used in this study (AN-reagent, 2% SDS, or 0.125 M NaOH). Given that these treatments do not allow for the conversion of cellulose I into cellulose II, the fiber structure shown in Figure 2.3 is highly unlikely to be accounted for by cellulose I microfibrils, the native form of cellulose. Typically, such a conversion is achieved by treatment with 2.25-8 M NaOH

in a process called mercerization, but not by any acidic conditions or less alkaline conditions like 0.125 M NaOH or SDS solution, as far as we can tell. It is accordingly hypothesized that the fibrillar structure of cellulose observed in this study is a much less stable form of cellulose than cellulose I microfibril probably owing to the failure of the crystallization/spinning process. The observed wavy contours of the fibers (Figure 2.6A), which were not observed in the case of some of the thinnest cellulose microfibrils ever reported (for example the one extracted from fruit parenchyma cell wall) (Niimura et al. 2010), also support this conclusion.

We then hypothesized that these fibers include fewer cellulose chains being extended. As a result, the conversion to cellulose II could be achieved by much milder treatment than mercerization. The resultant cellulose II appeared to consist of ellipsoidal globules tied in a row (Figure 2.5C, 2.5D and Figure 2.6B). Given the morphology, we propose two putative mechanisms for the conversion observed in this study (Figure 2.6): reprecipitation model and folding model. In the former model, shorter cellodextran chains, which were generated from the fiber structure by the chemical treatment for purification, reprecipitated on a longer core chain of cellulose, and then were crystallized into cellulose II-like structure (the upper mechanism in Figure 2.6C) as often seen for cellodextran molecules (Kobayashi et al. 2000). Such shish-kebab structure has been reported for cellulose (Buleon et al. 1977). The latter model is simply assuming the folding of cellulose polymer chains to realize the anti-parallel packing of cellulose II (Langan et al. 2001). Formation of the tied globules may occur as a result of folding of cellulose chains at several different points in a single fiber (the lower mechanism Figure 2.6C). Folding of cellulose chains in cellulose II crystal has been reported as well (Kuga et al. 1993; Shibazaki et al.1995).

2.3.4 Why we cannot reconstitute the native functionality of cellulose synthase?

As described, cellulose was not obtained in its native structural form despite the successful reconstitution of cellulose synthase in *E. coli*. Such partial denaturation of the enzyme was also observed for the *in vitro* synthesis of cellulose by a crude enzyme extracted from *G. xylinus* (Hashimoto et al. 2011). This may be due to the disruption of cells by lysis treatment. The current study aimed to address this hypothetical problem by expressing cellulose synthase in the cell membrane of *E. coli*. However, as shown here, the reconstitution of cellulose synthase in cell membrane of living *E. coli* is not sufficient for the complete reconstitution of cellulose synthase. This implies that neither membrane potential nor concentration gradients of any solutes fulfil the requirements for the native activity to synthesize cellulose microfibril.

What then, are the missing factors required for native cellulose synthase activity? One of the candidates is represented by the CesC and CesD proteins, which are clustered together with CesA and CesB in the same operon (Wong et al. 1990; Saxena et al.1994). CesD protein was reported to be responsible for crystallization (Saxena et al. 1994) and involved in the translocation of cellulose chains (Hu et al. 2010). Glycosyl hydrolase GH-8 and ccp2 protein, which are encoded upstream of the operon of interest, are also known to be involved in cellulose biosynthesis in *G. xylinus* (Nakai et al. 2013; Sunagawa et al. 2013). Given that these subunits are likely to play any roles in cellulose synthesis, reconstitution of cellulose I-synthesizing activity may need correct expression of all these proteins.

Another key factor may involve the formation of a terminal complex (TC) - a supermolecular cellulose synthase structure (Kimura et al. 1999; 2001). In *G. xylinus*, TC is the linear type, in which the complex is present in a row along the long-axis of the

cell (Kimura et al. 2001). The liner type TC is reminiscent of a linear arrangement of the magnetosome chain in magnetotactic bacteria, consisting of Fe_3O_4 magnetite particles queued up in the bacterial cell (Komeili et al. 2006; Scheffel et al. 2006). This chain structure is believed to be maintained by the cytoskeletal MamK protein interacting with the cytoskeleton and the magnetosome together with the MamJ protein (Frankel and Bazylinski 2006; Draper et al. 2011). The missing factor for native cellulose synthase activity may thus be the anchoring protein and the cytoskeleton beneath the cell membrane, and for this reason, further research in this field must aim to identify proteins that, like MamK, interact with both cellulose synthase and the cell cytoskeleton.

Despite not achieving native cellulose synthase activity, the system established and described here represents a convenient and efficient experimental approach to analyze the polymerization process of cellulose synthase. Furthermore, in order to understand the crystallization process, one can supplement this system with the missing candidate factors for reconstituting the native activity of cellulose synthase in *E. coli*. We have called this system CESEC (CEllulose-Synthesizing *E. coli*). In addition to the functional analysis of cellulose synthase, CESEC will allow for the development of novel cellulosic materials by virtue of the extremely fine cellulose fibers.

2.4 Summaries

We successfully reconstituted cellulose-synthesizing activity in *E. coli* by expressing cellulose synthase and DGC together, which we designated as CESEC. The cellulose synthesized by CESEC was extremely thin fiber probably due to the failure of crystallization. Given that it was converted to cellulose II aggregation by acid treatment

or milder alkaline treatment than ever known, this fiber is an unprecedented structure in which just a few chains of cellulose are bundled, rather than the native structure of cellulose, cellulose I microfibril. Despite of incomplete reconstitution of cellulose-synthesizing activity, CESEC will be a useful and easy tool for functional analysis of cellulose synthase by using recombinant protein.

FIGURE CAPTIONS

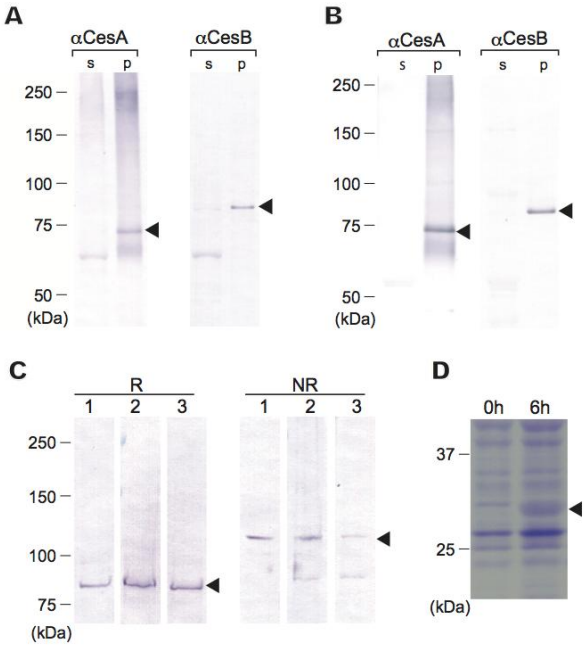

Figure 2. 1 SDS-PAGE analysis of recombinant proteins, LC/MS analysis of c-di-GMP, and cellulose quantification. Western blot analysis of alkaline fractionated sample of *E. coli* XL1-Blue transformants (A) and *G. xylinus* (B) stained with anti-CesA (αCesA) and anti-CesB (αCesB) antibodies. Lane s: soluble proteins (alkaline soluble fraction of cells); lane p: membrane proteins (alkaline insoluble fraction of cells). The arrowheads indicate the target bands of monomers. (C) Western blot analysis of whole cell samples of *G. xylinus* (lane 1) and *E. coli* (lanes 2-3) stained with αCesB antibody under reducing (R) and non-reducing (NR) conditions. Lane 1: *G. xylinus*; lane 2: *E. coli* XL1-Blue expressing CesA and CesB; lane 3: *E. coli* XL1-Blue expressing CesA, CesB, and DGC. (D) Whole cell samples of *E. coli* XL1-Blue before (0 h) and after (6 h) 6 h induction of protein expression were analyzed by staining with CBB. The arrowhead indicates the band of thioredoxin-fused DGC, which is detected only after induction.

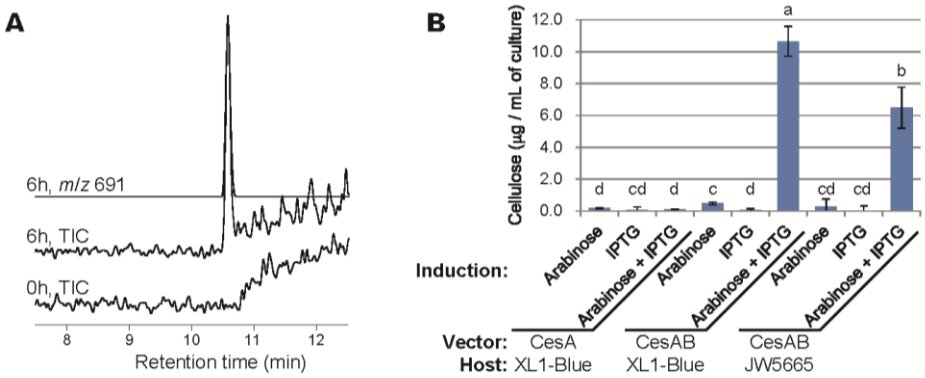

Figure 2. 2 Production of c-di-GMP and cellulose by the recombinant *E. coli*. (A) Mass chromatograms of LC/MS analyses of the cell extract. Total ion chromatogram (TIC) of positive polarity before (0 h, TIC) and after (6 h, TIC) induction are shown together with the mass chromatogram of *m*/*z* 691 in the positive polarity, corresponding to c-di-GMP, after induction (6 h, *m*/*z* 691). All ion chromatograms are shown in the same scale. (B) Quantification of the synthesized cellulose by the protocol of Updegraff (Updegraff 1969). Error bars represent standard deviation. The results of statistical analysis of the data are indicated by the alphabets (a to d) above each bar (p <0.01 by two-tailed Welch's t-test, N =3).

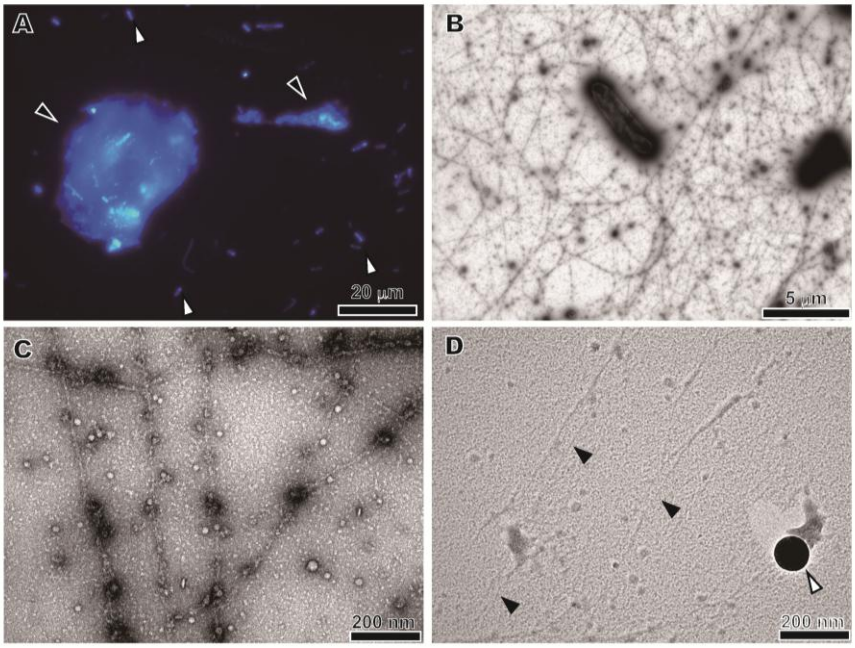

Figure 2.3 Microscopic observations of *E. coli* transformant cells. (A) Fluorescence micrograph of an *E. coli* sample stained with calcofluor-white. Black arrowheads indicate the strongly stained cocoon-like structures outside of the *E. coli* cells, which are weakly stained as indicated by white arrowheads. (B and C) Negatively stained *E. coli* cells expressing CesA, CesB, and DGC in lower (B) and higher (C) magnification. Massive production of fiber structures is observed around the cells. (D) The fiber structures observed by shadowing with casted Pt/Pd. Black arrowheads indicate fibrillar structures and white arrowheads indicate a polystyrene bead standard of 100 nm diameter.

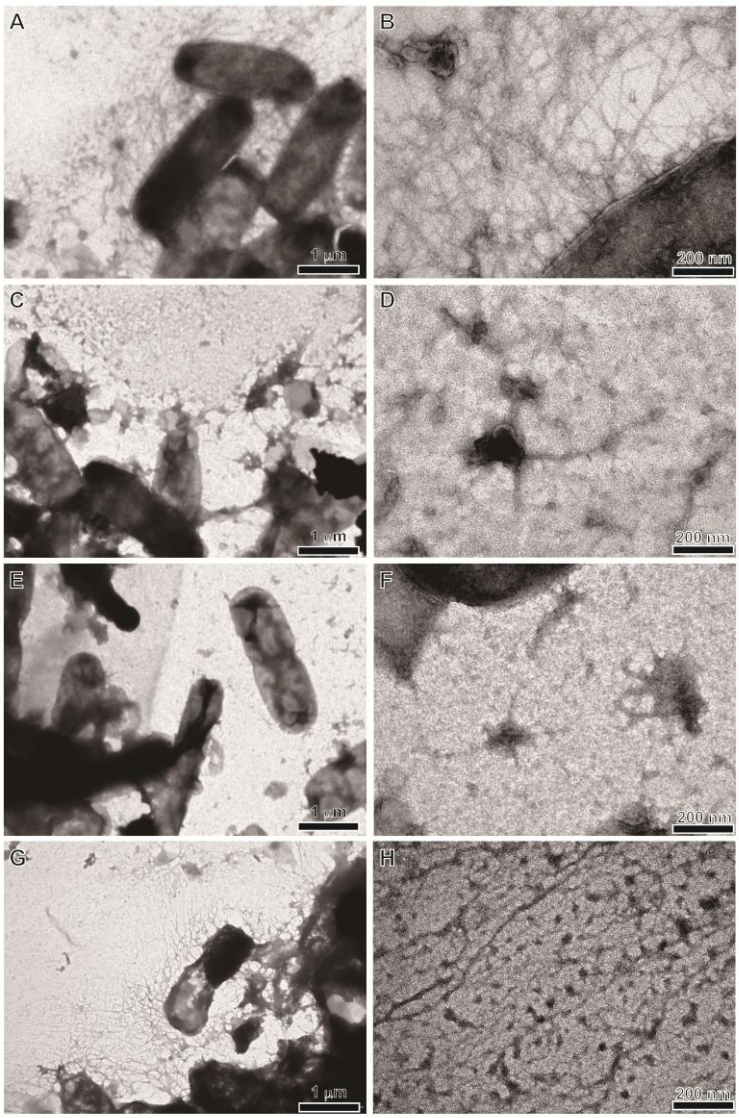

Figure 2.4 Electron microscopic observation of the cellulose fiber structures during cellulase digestion. The sample was treated with blank buffer (A, B), 0.1% cellulase (C, D), 0.5% cellulase (E, F), or 0.1% lysozyme (G, H).

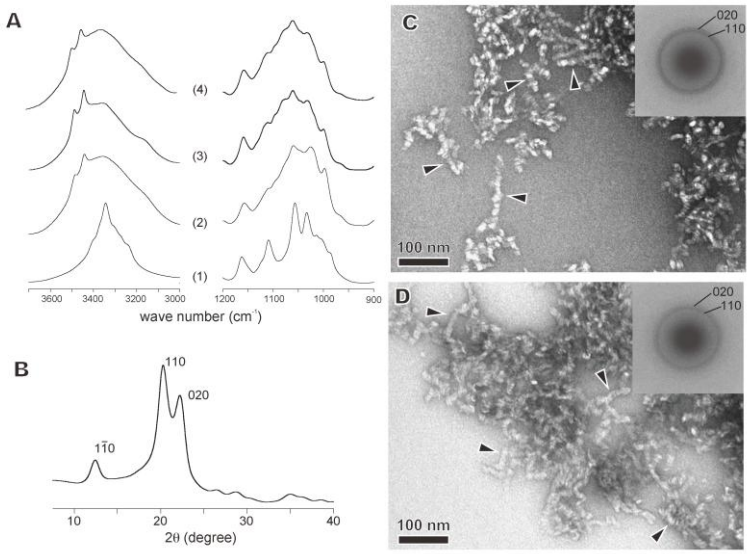

Figure 2.5 Characterization of the cellulose product synthesized by *E. coli* transformant cells after chemical treatment. (A) FTIR spectra of cellulose I standard (1: original bacterial cellulose), cellulose II standard (2: mercerized bacterial cellulose), and the product washed with AN-reagent (3) or SDS/NaOH (4). (B) X-ray diffraction pattern of a cellulose sample washed with SDS and NaOH. Diffraction peaks are clearly indexed by cellulose II crystal, as indicated. (C and D) Electron micrographs of negatively stained cellulose samples washed with AN-reagent (C) or SDS/NaOH (D). The arrowheads indicate characteristic globular structures tied in a row. The insets show electron diffraction diagrams together with indexing by cellulose II crystal.

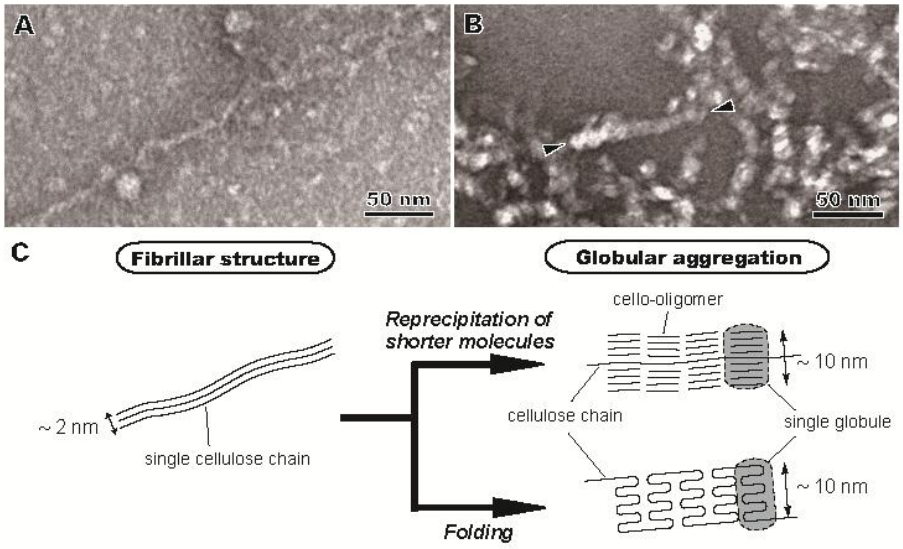

Figure 2.6 Putative models for the structural conversion from the nascent fibrillar structure (A) to globular aggregation (B). (A and B) Electron micrographs of negatively stained cellulose before (A) and after (B) AN treatment. The arrowheads in B indicate globular structures tied in a row. (C) Schematic diagrams of the structural conversion of cellulose observed in this study. Considering the smallest dimension of the fiber before washing, and given that milder chemical treatment than ever described before was enough to convert the fibrillar structure (A) to globular cellulose II aggregations (B), it is hypothesized that extremely low numbers of cellulose chains are packed in each of the single fibrillar structures. Such structures would not be resistant to chemical treatment with AN-reagent, SDS or diluted NaOH solution, and subsequently may be converted to globular structures tied in a row by either reprecipitation of shorter chains on the long core chain or folding at multiple sites.

Chapter 3 Functional analysis of cellulose synthase by site-directed mutagenesis

3.1 Introduction

Cellulose is a structural polysaccharide produced by plants, algae, protists, bacteria, and animal tunicates, and one of the most abundant biological polymers on Earth. Cellulose biosynthesis is actually a two-step reaction of (i) polymerization of β1→4-glucan and (ii) crystallization of the resulting polymers (microfibril formation). The enzyme responsible for cellulose biosynthesis is cellulose synthase, which is embedded in the lipid bilayer of cell membranes and is believed to be a heterosubunit complex. Therefore, it has been a difficult protein to analyze, and our biochemical understanding of cellulose biosynthesis remains limited.

The gene encoding the catalytic subunit of cellulose synthase is *cesA* (Delmer 1999; Somerville 2006). The CesA protein is a glycosyltransferase of the GT-2 family according to the CAZy database. Other polysaccharide synthases are present in the GT-2 family including chitin synthase, β1→3-D-glucan synthase, mannan synthase, and hyaluronan synthase. Hydrophobic cluster analysis of amino acid sequences in an earlier study clarified that these β-glycosyltransferases have two domains (domains A and B), which contain D, D and D, QxxRW sequences, respectively (Saxena et al. 1995). The function of these highly conserved motif sequences was discussed in that study, for example, domain B was proposed to be important for chain elongation since it was

found only in polysaccharide synthases. However, only a few studies (Nagahashi et al. 1995; Saxena and Brown 1997; Dorfmueller et al. 2014) directly showed that these amino acid residues are involved in polysaccharide synthesis.

Recently, the X-ray crystallographic structure of cellulose synthase was reported from the minimally required subunits of bacterial cellulose synthase, CesA and CesB, of the purple bacterium *Rhodobacter sphaeroides* (Morgan et al. 2013; 2014; 2016); hereafter, we use the terminology proposed by Delmer (CesA) (Delmer 1999), instead of the original name (BcsA), which was also used other recent studies (Morgan et al. 2013; 2014; 2016). This is the first three-dimensional structure determination, not only of cellulose synthase, but also for a GT-2 enzyme carrying domain B. This structural model clearly indicates that the two aforementioned aspartic acid residues in domain A are involved in the interaction with the UDP (uridine diphosphate) moiety of the substrate UDP-glucose, and the aspartic acid in domain B functions as the catalytic base in the glucosyltransfer reaction. The famous QxxRW motif in domain B, located in an interfacial α-helix (IF2) running on the inner surface of the lipid bilayer, plays an important role for keeping acceptor cellulose molecules in the correct position for the glucosyltransfer. In addition to these well-known motifs, the structural model of cellulose synthase indicated other important motifs in CesA, such as QTPH and FFCGS. Both of these are close to the acceptor cellulose chains and are proposed to play an important role in glucosyltransfer or chain translocation.

Despite such outstanding structural models that tell us new information about the mechanism of cellulose synthase, it is still important to test the molecular mechanism of cellulose synthase deduced from the X-ray crystallographic structure by observing its enzymatic activity. Site-directed mutagenesis is a clear way to evaluate the role of each

amino acid residue in cellulose synthase. Although several previous studies have surveyed the effect of mutating the D,D,D,QxxRW motif in cellulose synthase (Saxena and Brown 1997) and chitin synthase (Nagahashi et al. 1995; Dorfmueller et al. 2014), the mutations in these studies were actually designed based on amino acid sequence alignment (Saxena et al. 1995).

In this study, we designed site-directed mutagenesis of the bacterial CesA protein with the aid of the recently published structural model of the RsCesAB complex (Morgan et al. 2013; 2014; 2016). Then, we determined the cellulose-synthesizing activity for each of these mutants by expressing bacterial cellulose synthase in recombinant *Escherichia coli*, which is designated as "CESEC" (cellulose-synthesizing *E. coli*) (Imai et al. 2014). Our results were consistent with these structural studies, and further suggest that the sulfur-arene interaction around the cysteine residue in the FFCGS motif is key for CesA protein function.

3.2 Materials and Methods

3.2.1 Bacterial strains and plasmids

CESEC (Imai et al. 2014) was used for assaying recombinant cellulose synthase enzymatic activity. Briefly, the *E. coli* strain XL1-Blue was used for expressing cellulose synthase derived from *Gluconacetobacter xylinus* JCM9730 (GxCesA and GxCesB, the minimal requirement for cellulose-synthesizing activity in bacteria). The *gxcesA* and *gxcesB* genes, which are in two sequential open reading frames in the same operon, were inserted into a pQE-80L vector (Qiagen Inc.) for their expression. In addition, DGC (diguanylate cyclase) was expressed together with cellulose synthase. Diguanylate cyclase is an enzyme that synthesizes c-di-GMP (cyclic-di-guanosine

monophosphate), an activator of bacterial cellulose synthase (Ross et al. 1987; Omadjela et al. 2013). The *dgc* gene of *Thermotoga maritima* MSB8, TM1788 (Rao et al. 2009) , was inserted into a pBAD33 vector for expression as a thioredoxin-fused protein. These two vectors were introduced into *E. coli* by chemical transformation, and the transformed *E. coli* were selected using the antibiotics ampicillin and chloramphenicol, resistance to which was induced by the pQE-80L and pBAD33 vectors, respectively.

3.2.2 Site-directed mutagenesis

A series of site-directed mutagenesis experiments were performed on the *gxcesA* gene in a sub-cloning vector pGEM-T easy (Promega Inc.) using a QuikChange Lightning site-directed mutagenesis kit (Agilent Technologies Inc.), according to the manufacturer's protocol. DNA sequences were verified for the desired mutagenesis, and then the mutated sequence was cut out at the endogenous restriction sites (*EcoR*I sites for D188H, D188N, D189N, and D189Y, and *BsrG*I and *Sac*II sites for the others). The expression vector containing cellulose synthase (GxCesA and GxCesB) was digested at the same restriction sites for each mutant. Mutated *cesA* DNA fragments were then ligated to the expression vector by using a DNA Ligation kit LONG (Takara Bio Inc., Japan). The ligated plasmid DNA was amplified in *E. coli* HST08 (Takara Bio Inc.) to prepare the expression vector of cellulose synthase containing a particular point mutation. The orientation of the ligated DNA fragment was verified by colony-direct PCR for D188H, D188N, D189N, and D189Y.

3.2.3 Expression of recombinant proteins

CESEC cells were cultured in 2 × YT medium supplemented with 12.5 μg/mL tetracycline, 100 μg/mL ampicillin, and 50 μg/mL chloramphenicol at 37°C with orbital shaking at 190 rpm. Protein expression of cellulose synthase and DGC was induced with 0.4 mM IPTG and 0.2% L-arabinose, respectively, when the OD_{600} reached 0.5-0.7. The culture was then maintained with orbital shaking at 28°C prior to harvesting by centrifugation. The wild type CesA was expressed alongside mutant proteins to compare protein expression and cellulose production for each mutant protein.

3.2.4 Western blot analysis

Expression of GxCesA and GxCesB was analyzed by SDS-PAGE and western blotting. Cultured cells were collected by centrifugation at 4°C, and then incubated in SDS-PAGE sample buffer (50 mM Tris-HCl (pH 6.8), 0.5% SDS (sodium dodecyl sulfate), 2% β-mercaptoethanol, 10% glycerol, and 0.01% bromophenol blue) at 4°C for at least 3 hours. Proteins included in the cells in 24 μL culture medium were analyzed with a precast 10-20% polyacrylamide gel (SuperSep Ace, Wako Pure Chemicals Industries Ltd., Japan) alongside a molecular weight marker (Precision Plus Protein All Blue Standards, Bio-Rad Inc.), and transferred onto PVDF membranes (Immobilon-P, Millipore Inc.). The membrane was then incubated with a primary antibody against either GxCesA or GxCesB. The antibodies used were described in our previous studies (Imai et al. 2014; Hashimoto et al. 2011) (a polyclonal antibody against a synthetic peptide corresponding to the carboxyl terminus of GxCesA and a loop in the CBD2 domain of GxCesB protein (Morgan et al. 2013), respectively). Membranes were then incubated with anti-rabbit IgG conjugated to horseradish peroxidase (Promega Inc.).

Bands of CesA and CesB protein were visualized by a chemiluminescence method to quantitatively evaluate the expression of CesA and CesB proteins. ECL Select (GE Healthcare Inc.) was used for the luminescence reaction and digital images were taken by AE-9300H EZ-Capture MG (ATTO Inc., Japan). The intensity of CesA and CesB bands, which represents the amount of protein in the cells included in 24 μL of culture medium, was determined by ImageJ. Expression of GxCesA and GxCesB protein in each mutant cellulose synthase was evaluated as a percentage relative to wild type, hereafter referred to as the relative expression level.

To verify the correct expression of GxCesA and GxCesB protein, we examined samples prepared by alkaline fractionation, (Ito et al. 1991) which separates the membrane-spanning proteins from other proteins. Briefly, cells treated by lysozyme were solubilized in 0.1 N NaOH solutions on ice for 30 min and ultracentrifuged at 100,000 $\times g$ for 30 min. The pellet, containing membrane proteins, was washed with 5% trichloro acetic acid (TCA), whereas the proteins in the supernatant, including unfolded proteins and soluble proteins, are precipitated by adding TCA in a final concentration of 10%. These precipitated protein samples were air-dried after washing with cold acetone, and then were dissolved in 1% SDS, 50 mM Tris-HCl (pH 8.0), 1 mM EDTA for subsequent SDS-PAGE and western blot analysis.

3.2.5 Isolation and quantification of synthesized cellulose

Cellulose synthesized by *E. coli* was isolated and quantified as previously described (Imai et al. 2014). Briefly, the centrifuged pellet of culture medium was incubated at 100°C for 30 min in a mixture of glacial acetic acid and concentrated nitric acid (volume ratio of 8:1, hereafter referred to as AN-reagent). The remaining precipitate

was used for quantifying cellulose content by the anthrone-sulfuric acid method as previously described. (Imai et al. 2014) Negative values were treated as zero grams of cellulose. Three independent experiments were performed for each mutant, and statistical tests (Welch's *t*-test) were done by the built-in function of Microsoft Excel (TTEST) to compare cellulose content produced by each construct. Estimated values of the cellulose production per mL of culture in each mutant were normalized to the relative CesA expression level of the mutant to wild type, which was estimated by quantitative western blot analysis as described in 3.2.4. Normalized cellulose production was accordingly indicated as a percentage relative to wild type.

3.2.6 Structural analysis of synthesized cellulose

Cellulose in the culture medium was isolated by chemical washing with AN-reagent, as described in 3.2.5. The residue, after repeated washings with water, was analyzed by electron microscopy, electron/X-ray diffraction, and Fourier-transformed infrared spectroscopy (FTIR). Samples were prepared for electron microscopy and electron diffraction on a thin carbon-coated copper mesh. The mesh for electron microscopy was stained with 2% uranyl acetate. A JEM-2000EXII (JEOL Co. Ltd., Japan) was used for both electron microscopy and electron diffraction. Electron micrographs were taken with a CCD camera (MegaView G2; Olympus Soft Imaging Solutions GmbH), and electron diffraction diagrams from a 1-μm diameter region, which was probed by exciting the first condenser lens maximally, were recorded on photographic emulsion films (Kodak SO-163) and developed by Kodak D-19 with full strength by following the manufacturer's protocol. The obtained diffraction patterns were calibrated by a diffraction ring from the (111) plane of gold (d = 0.2355 nm).

For X-ray diffraction, washed samples were lyophilized and pressed to make a tablet. X-ray of Ni-filtered Cu Kα generated by a rotating anode (RU-200BH, Rigaku Inc., Japan) operated at 50 kV and 100 mA was collimated with a 0.3 mm-diameter pinhole and directed to the sample tablet. Wide-angle diffraction patterns were recorded on imaging plates (BAS-IP SR 127, Fujifilm Corp., Japan) with a vacuum camera. Camera length was calibrated using NaF powder (d = 0.23166 nm).

Spectrum One or Frontier (Perkin Elmer Inc.) was used for FTIR analysis with attenuated total reflection (ATR) attachment. The sample in water was dried on a diamond ATR probe by nitrogen gas, and then spectra were taken with 4 cm^{-1} resolution and 16 integrations in the range of 4000-400 cm^{-1}.

3.3 Results

3.3.1 Optimizing conditions for functional analysis of cellulose synthase by CESEC

Prior to analyzing cellulose production by CesA mutants in CESEC, we first determined the optimal duration for expressing cellulose synthase in *E. coli*. The amount of cellulose produced increased for up to 6 h after induction and stayed constant up to 19 h in wild type cellulose synthase (Figure 3.1A and Figure 3.2). We examined cellulose production at 6 h of induction to evaluate the activity of cellulose synthase over long durations, which is a good indication of a full yield of cellulose production by recombinant GxCesAB in living cells.

We also estimated the cellulose production yield normalized to the amount of cellulose synthase expressed. The expression of GxCesA and GxCesB proteins typically reached a maximum at an earlier stage, 2 h after induction, and then gradually

attenuated, whereas the synthesized cellulose accumulated up to 6 h after induction as described above (Figure 3.1). We analyzed samples at 2 h after induction to correctly normalize cellulose production by cellulose synthase level, given that the relationship between cellulose production and protein expression level at 4 h or later during induction is too complicated to interpret. The level of CesA protein was used for normalizing cellulose production as a percentage to wild type (% of WT) as CesA is a core catalytic subunit of cellulose synthase.

We also analyzed GxCesA and GxCesB protein expressed in *E. coli* by alkaline fractionation (Ito et al. 1991), which separates membrane proteins as the alkaline-insoluble fraction from the other proteins in the alkaline-soluble fraction. For the mutant proteins tested in this study, western blot analysis revealed that both CesA and CesB proteins were found only in the alkaline-insoluble fraction (Figure 3.4), although some mutants showed a very weak signal due to a low expression level. We then concluded that, despite the introduced mutation, GxCesA and GxCesB proteins are correctly expressed in *E. coli* cell membranes.

3.3.2 Mutation of D,D, and D,QxxRW motifs

Amino acid sequence analysis of CesA indicated the presence of two highly conserved motifs in cellulose synthases and some polysaccharide synthases: the D,D motif and D,QxxRW motif (Saxena et al. 1995) . Recent X-ray crystallographic analyses clearly revealed that these motifs are located in the active site of cellulose synthase (Morgan et al. 2013; 2014). Given that these sequences are well conserved in CesA proteins (Figure 3.3), we conducted site-directed mutagenesis experiments to

inactivate these amino acid residues. The prepared mutant GxCesA proteins were expressed together with wild type GxCesB and DGC.

As expected, most of the inactivating mutants of GxCesA showed significantly reduced cellulose production compared with wild type GxCesA protein as observed by cellulose production at 6 h after induction (full yield), while no significant difference from wild type was found only for the M371A mutant among those tested in this study (Figure 3.5A and Table 3.1, $P = 0.066$ by Welch's *t*-test). Normalized cellulose production also showed that most mutants tested here, except for D189Y and M371A, were clearly inactive (Figure 3.5C). We will not discuss the high normalized cellulose production for D189Y as this could be erroneous because of extremely low expression of CesA (Figure 3.5B). On the other hand, M371A showed significant cellulose production and enough cellulose was successfully collected for structural analyses as shown in 3.3.5 This result is reasonable given that, in this mutation, a less-conserved amino acid (the third residue in the QxxRW motif of CesA, see Figure 3.3) was replaced by alanine, which is in general less detrimental for protein structure. Substantial cellulose production was also observed for other mutants in our preliminary data (for example P265A, or *N*/*C*-terminal deletion mutant; data will be shown elsewhere). This clearly means that the cellulose-synthesizing activity in our system can persist when the mutation is not detrimental, and therefore decreased cellulose production in our system is due to decreased activity of the mutant cellulose synthase.

3.3.3 The cysteine side chain in the FFCGS motif is important for function

In addition to the highly conserved sequence motif of D, D, D, QxxRW, the X-ray crystallographic structure newly revealed an important motif sequence in CesA, the

FFCGS motif (Morgan et al. 2013). The cysteine residue in this motif, which lies at the entrance of transmembrane channel, seems to interact with the glucopyranose residue at non-reducing end of the growing chain by using its main chain carbonyl (Morgan et al. 2013). We tested this hypothesis by mutating this cysteine in the FFCGS motif. Given that the main chain of this cysteine is involved in the proposed interaction, the cysteine could be exchanged to any other amino acid unless largely disturbing the tertiary structure. We then analyzed GxCesA mutants in each of which the corresponding cysteine (C308) was mutated to either of alanine, phenylalanine, histidine, methionine, proline, serine, threonine, or valine.

As shown in Figure 3.6A and 3.6C and Table 3.1, all eight GxCesA-C308X mutants tested in this study did not show cellulose production upon expression in CESEC as measured by full yield or normalized production. It is interesting that C308S, in which the side chain sulfur is replaced by oxygen, showed no cellulose production despite substantial expression of GxCesA and GxCesB, suggesting the absolute importance of the cysteine side chain in the FFCGS motif. Furthermore, the C308M mutant showed very little activity, indicating that a sulfur in the side chain is not sufficient for activity. These results suggest that the thiol side chain of cysteine in the FFCGS motif is strictly required for the function of cellulose synthase.

3.3.4 Sulfur-arene interaction may be involved in cellulose synthesis

In order to examine how the cysteine thiol group in the FFCGS motif is involved in cellulose synthase, several other mutants of GxCesA were examined. For all six PDB models deposited (PDB ID: 4HG6, 4P00, 4P02, 5EJ1, 5EIY, and 5EJZ), three aromatic amino acid residues are found around this cysteine (F301, Y302, and F316 for CesA of

R. sphaeroides (RsCesA), see Figure 3.3 and 3.4). These residues appear to form a pocket surrounding the side chain thiol of cysteine, and the distance between the thiol and the aromatic ring is around 4 Å. An interaction between sulfur and aromatic rings, called a sulfur-arene interaction, is sometimes found in protein structures and protein-ligand interactions (Duan et al. 2001; Salonen et al. 2011). To determine if such interactions take place within GxCesA, we performed site-directed mutagenesis on those aromatic amino acid residues (F291, Y292, and F306 in GxCesA, see Figure 3.3) systematically changing each to an alanine. Single mutations (F291A, Y292A, and F306A) and double mutations (F291A/Y292A, F291A/F306A, and Y292A/F306A) of GxCesA drastically reduced cellulose production compared to the wild type enzyme (Figure 3.6). Therefore, these three aromatic ring amino acids were essential for cellulose synthesis. Finally, no significant cellulose production was observed by GxCesA-C308V and C308F mutants (Figure 3.6 and Table 3.1), indicating that a hydrophobic side chain cannot replace the cysteine residue in the FFCGS motif. All these data support the importance of the cysteine side chain thiol at this residue, and we then propose that a sulfur-arene interaction plays a role to place the cellulose molecular terminal at the correct position for successive glucosyltransfer.

3.3.5 Structural analysis of the cellulose produced by a mutant CesA protein

In this study, we found a mutant CesA protein whose activity was not abolished, i.e. M371A. Electron microscopy, electron/X-ray diffraction, and FTIR analysis revealed that the product of this CesA M371A mutant was a globular aggregation crystallized into cellulose II polymorph after chemical washing, as well as that by the wild type (Figure 3.8). Electron diffraction diagrams showed two diffraction rings of cellulose II

crystal lattices ((110) and (020)) (Langan et al. 2001), but diffraction from $(1\,\bar{1}\,0)$ was not confirmed. This rules out that cellulose chains are short enough to let themselves stand perpendicularly on the electron microscopic supporting film, which would allow all these three diffractions to be generated as previously observed in the case of reversing cellulose (Kobayashi et al. 2000) or cellobiose phosphorylase reaction (Hiraishi et al. 2009). Given this result, the synthesized cellulose is probably a polymer long enough to be laid down on the supporting film in both wild type and M371A. These structural characteristics are consistent with our previous studies reported for CESEC (Imai et al. 2014) and *in vitro* synthesized cellulose by crude enzyme extracts of *G. xylinus* (Hashimoto et al. 2011).

3.3.6 Mutation the QxxRW motif of bacterial cellulose synthase to plant-type sequence

By addition, QxxRW is one of the highly conserved motifs in CesA proteins, and it has demonstrated to have interactions with the terminal portion of the cellulose chain (Morgan et al. 2013) and UDP (Morgan et al. 2013). Closer investigation of these motif sequences, however, shows that plant CesA has a consistently different sequence of QVLRW, whereas QRxRW is found in the bacterial and tunic CesA. Given this fact, we were then interested in whether the plant-type QVLRW motif is functional in bacterial cellulose synthase. GxCesA-R370V/M371L double mutant (QVLRW mutant), estimated with CESEC, exhibited no significant production of cellulose (Table 3.1 and Figure 3.9). As we cannot get all the expression of these mutations by alkaline fractionation methods, only got the expression by western blot and visualized by chemiluminescence method. And the amount of cellulose was quantified at 6 hours.

These results demonstrate that plant-type QxxRW motif may be not function in bacterial CesA. In the structural model of bacterial cellulose synthase, the second residue in QxxRW (R380) forms salt bridge to E297, which is majorly replaced by arginine in plant-type CesA (Figure 3.7). Subsequently, an E287R mutation was added to the QVLRW mutant to prepare a triple mutant E287R/R370V/M371L as the putative plant-type architecture, and quantified cellulose production for this mutant. Again, no significant activity was observed for this triple mutation as well as each of single mutation of E287 to alanine (E287A) and arginine (E287R). In summary, the architecture of bacterial cellulose synthase around the QxxRW motif is sufficiently strict so as to not allow substitution of the plant-type sequence (QVLRW).

3.4 Discussions

3.4.1 CESEC as a platform for the functional analysis of cellulose synthase

This study functionally analyzed cellulose synthase by using recombinant protein with site-directed mutagenesis, and demonstrated that a point mutation in CesA can alter its enzymatic activity. These mutant proteins were correctly expressed by *E. coli* despite the introduced mutation as shown in Figure 3.4. This study putatively concluded that lower cellulose production by mutant cellulose synthases in this study was due to loss of enzyme function.

Given that cellulose synthase reconstituted in living *E. coli* cells was used, this study evaluated enzymatic activity in the cell membrane of a living cell, which is subjected to membrane potential, proton motive force, and solute concentration gradients between the extra- and intracellular space. This is significantly different from *in vitro* assays, which analyze membrane proteins whose extracellular and cytosolic sides are exposed

in the same solution environment unless additional techniques are used. This study therefore discusses the structure-function relationship of cellulose synthase in living cells, based on the reported structural models (Morgan et al. 2013; 2014; 2016) , and accordingly provides important information in addition to *in vitro* assays, which have the advantage of being amenable to controlling reaction conditions (pH, ligand concentration, temperature, and other parameters).

We however must acknowledge that the reconstituted activity in *E. coli* is not yet able to produce the native cellulose structure (cellulose I microfibril) as shown in Figure 3.8 and our previous study (Imai et al. 2014). On the other hand, it was shown that the DP (degree of polymerization) of cellulose synthesized by CESEC was as high as 700 (Imai et al. 2014). This indicates that the activity reconstituted in *E. coli* cells, which was analyzed in this study, accomplishes the polymerization function but not crystallization. Loss-of-function mutants observed in this study then probably can be described as mutants deficient in polymerization. This is currently the limitation for using CESEC to analyze the enzymatic activity of cellulose synthase.

3.4.2 A sulfur-arene interaction is involved in cellulose biosynthesis

An unexpected result in this study was that the cysteine residue in the FFCGS motif was not amenable to any mutation examined (i.e., neither alanine, serine, threonine, nor methionine can replace this cysteine and maintain enzyme activity). We then hypothesized that sulfur-arene interactions between the cysteine side chain thiol in the FFCGS motif and the surrounding aromatic side chains of phenylalanine and tyrosine in the IF1 helix are responsible for controlling enzyme activity (Figure 3.10). These residues (F301, Y302, F316, and C318 in RsCesA) appear to be located in a similar

position in all the six available models (Morgan et al. 2013; 2014; 2016). This indicates that the IF1 helix and the cysteine in the FFCGS motif operate together even in different states. We then propose that the aromatic residues in the IF1 helix associates with the cysteine side chain in the FFCGS motif by sulfur-arene interaction, which is required for placing the main chain carbonyl of the cysteine residue adequately for the successive glucosyltransfer at the molecular terminus of cellulose. The importance of this sulfur-arene interaction is notably unusual, given that this interaction is not as common as hydrogen bonding, electrostatic interactions, or hydrophobic interactions.

As suggested by Morgan (Morgan et al. 2013) , W383 in the QxxRW motif of the IF2 helix appears to interact with the glucopyranose ring of cellulose through CH-π stacking, and Y302 in IF1 seems to make hydrogen bonds with the terminal glucose of growing cellulose chain in the c-di-GMP binding state (Morgan et al. 2014) . These structural models also demonstrate that the terminus of the growing cellulose chain is interposed between the IF1 and IF2 helices (Morgan et al. 2013). Furthermore, a closer look at the structural model suggests that F301 in the IF1 helix, a counter part of Cys 308 involved in the sulfur-arene interaction proposed in this study, has a CH-π stacking interaction with the glucopyranose ring next to W383 (Figure 3.10). These structural observations suggest the importance of IF1 and IF2 helices for CesA cellulose-synthesizing activity. Given the sulfur-arene interaction between the IF1 helix and the FFCGS motif, it is proposed that IF1, IF2, and FFCGS motifs are functionally connected, and interact with both UDP and cellulose (Figure 3.10). As proposed previously (Morgan et al. 2013), the cysteine in FFCGS and the tryptophan in QxxRW play a role in cellulose translocation. Our model supports this hypothesis and furthermore indicates that these two residues operate together in cellulose translocation. The cooperative action of the proposed unit

in Figure 3.10, which has multiple interactions with UDP-glucose and cellulose, is likely to account for a part of successive glucosyltransfer mechanism including cellulose translocation, as well as the finger helix movement as shown *in crystallo* (Morgan et al. 2016).

3.4.3 Introduced mutation could modulate the structure of produced cellulose?

This study showed that GxCesA-M371A still maintains significant activity. However, this is in contrast to a recent report on another GT-2 enzyme, NodC, which synthesizes chitin. The L279A mutant of NodC (an alanine mutation in the third residue of the QxxRW motif), which is equivalent to CesA-M371A in this study, did not exhibit any activity when expressed as a recombinant protein. (Dorfmueller et al. 2014) This implies that mutations in this residue modulate GT-2 enzymes including CesA protein to varying degrees. A closer look at our FTIR data actually revealed that cellulose synthesized by CesA-M371A mutant showed a slightly different IR spectrum in the fingerprint region around 1050 cm^{-1}, as shown in Figure 3.8D (the right part of spectra in the figure), indicating that this mutation might modulate the cellulose-polymerizing activity of CesA. Future studies will attempt to explain this difference in cellulose structure for properties such as molecular weight. Accumulating such data with several mutants will shed more light on the mechanism of cellulose synthase.

3.4.4 Plant-type sequence in the QxxRW motif cannot replace the corresponding part of bacterial cellulose synthase

Replacement of the GxCesA QxxRW motif (QRMRW) with the plant-type sequence (QVLRW) resulted in a loss of cellulose synthesizing activity. This may indicates that

plant CesA possesses a different mechanism for cellulose synthesis than bacterial CesA. For clearly address this conclusion, more efficient culture conditions are required for getting more expression of CesA and CesB. In addition, the X-ray crystallographic model clearly demonstrated that the first residue (i.e., glutamine) and the fifth residue (i.e., tryptophan) in the highly conserved QxxRW motif interact with substrate and acceptor, respectively (Morgan et al. 2013; 2014). Given that these interactions are involved in the catalytic reaction of cellulose synthase, the function of the QxxRW motif proposed for bacterial CesA is probably shared by all CesA proteins. We then hypothesized that this motif is regulated in a different way between bacteria and plants, due to which the plant-type sequence is not functional in bacterial CesA architecture.

Interfacial helices of IF1 and IF2 thus have multiple interactions with cellulose and are directly connected by a salt bridge between E297 and R380 in the same molecule (Morgan et al. 2013). Given that plant CesA would also possess an IF1 and IF2 helix as suggested by the sequence alignment (Figure 3.3), it is supposed that plant CesA has a similar cooperative operation of IF1 and IF2 helices for cellulose synthesis. However the link between IF1 and IF2 in plant CesA is probably made in a different manner than for bacterial CesA, since the residues forming the bridge between IF1 and IF2, E297 and R380 for RsCesA, are bacteria specific (Figure 3.3). This could account for the loss-of-function of CesA carrying the plant-type QxxRW motif (QVLRW mutant). One of the ways to clarify how IF1 and IF2 in plant CesA are connected will be finding additional mutations to the QVLRW mutant, which can rescue the activity on CESEC.

3.5 Summaries

This study provides a functional analysis of cellulose synthase in living cells. Further studies using this system will deepen our understanding of cellulose biosynthesis. For example, implementing random mutagenesis and the rational design of specific mutations should provide further insight. On the other hand, *in vitro* assays have the advantage of being able to control the concentration of related molecules such as the substrate, activators, or any other ligands or cofactors. Such *in vitro* assays are necessary for analysing enzyme kinetics, which will provide important insights into the molecular mechanism of cellulose biosynthesis. Given that using CESEC is simple, CESEC will provide complementary information to *in vitro* assays, and will be a powerful tool for studying cellulose biosynthesis.

FIGURE CAPTIONS

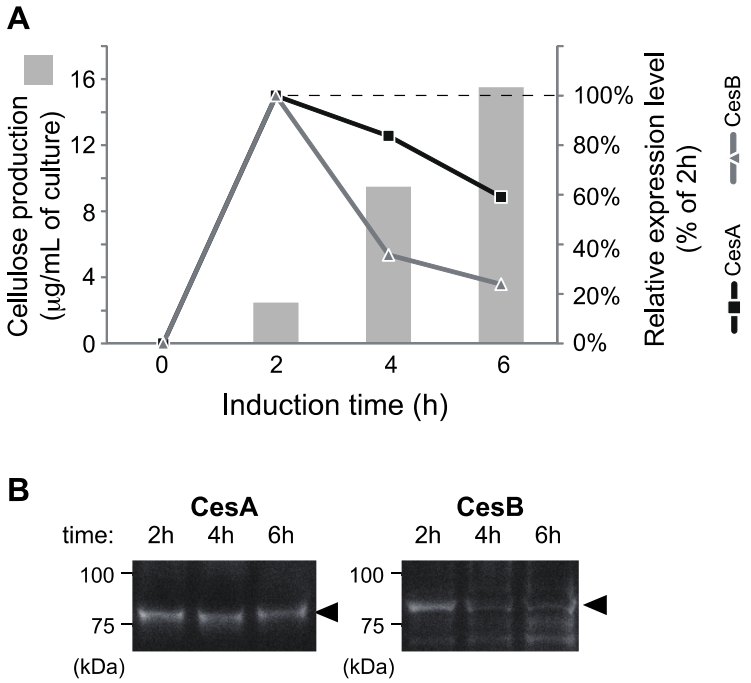

Figure 3.1 (A) Accumulation of cellulose produced by CESEC and relative expression level of GxCesA and GxCesB protein over time after inducing protein expression. Protein expression at 2 h of induction is set to 100% for both GxCesA and GxCesB. **(B)** Representative western blot analysis, which was used for plotting expression levels in panel A. Arrowheads indicate the target band.

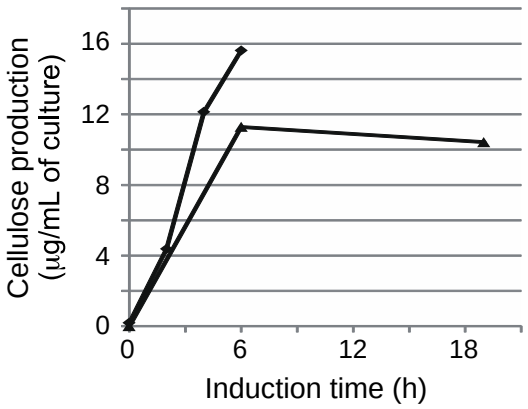

Figure 3.2 Accumulation of cellulose produced by wild type recombinant GxCesAB in other two independent CESEC experiments. Note that cellulose found at 19 h induction is nearly same as that at 6 h induction.

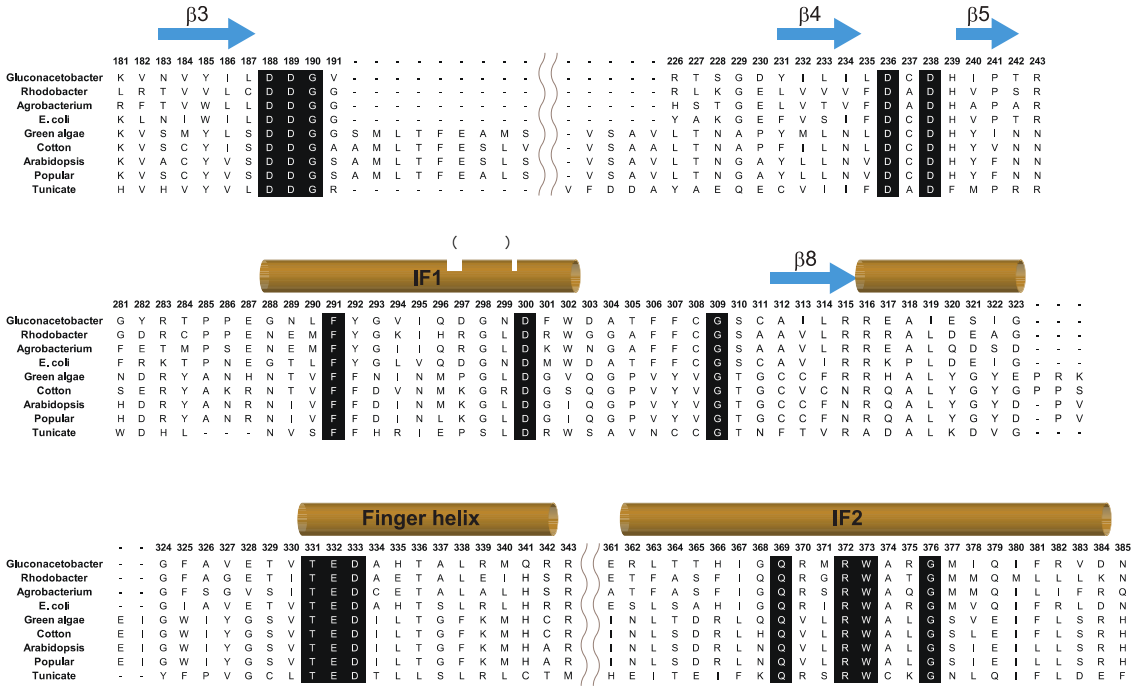

Figure 3.3 Alignment of prokaryotic and eukaryotic CesA amino acid sequences by MUSCLE. The analyzed sequences were from four bacteria, four plants including green algae, and one animal (tunicate). Gluconacetobacter: *G. xylinus* (GenBank ID: AB010645); Rhodobacter: *R. sphaeroides* (GenBank ID: CP000143.1); Escherichia: *E. coli* K12 (GenBank ID: NP_417990); Agrobacterium: *A. tumefaciens* (GenBank ID: AAC41436), Arabidopsis: *A. thaliana* (GenBank ID: NP_194967), Cotton: *Gossypium hirsutum* (GenBank ID: AAL37718), Green algae: *Micrasterias denticulata* (GenBank ID: ADE44904); Populus: *Populus tremuloide* (GenBank ID: AAO25536), Tunicate: *Ciona intestinalis* (GenBank ID: NP_001041448). The residue number of the *G. xylinus* sequence is indicated above the sequence, and the secondary structure revealed by X-ray crystallographic analysis of RsCesA is indicated on the top: orange cylinders and blue arrows stand for α-helix and β-sheet, respectively.

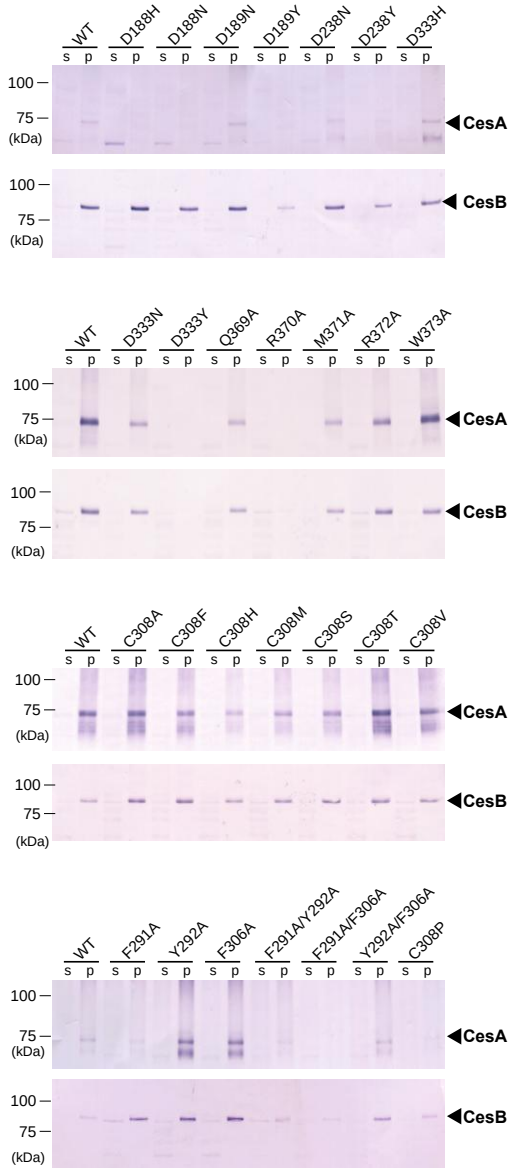

Figure 3.4 Western analysis of protein samples prepared by alakaline fractionation (Ito K, Akiyama Y 1991) for *E. coli* cells expressing GxCesA and GxCesB. The cells equivalent to 40 μL culture were analyzed in each lane by SDS-PAGE using precast gel (5/20% gradient gel of SuperSep Ace, Wako Pure Chemicals Industries Ltd., Japan), and blotted to nitrocellulose membrane and visualized by alkaline phosphatase-conjugated secondary antibody. Alkaline soluble and insoluble part is indicated by "s" and "p", respectively. The soluble part includes soluble proteins and misfolded proteins in the case, while the insoluble part includes membrane-anchored proteins. It is shown that both GxCesA and GxCesB were expressed in cell membrane for all the cases here, supporting the correct expression of cellulose synthase in mutants as well as wild type.

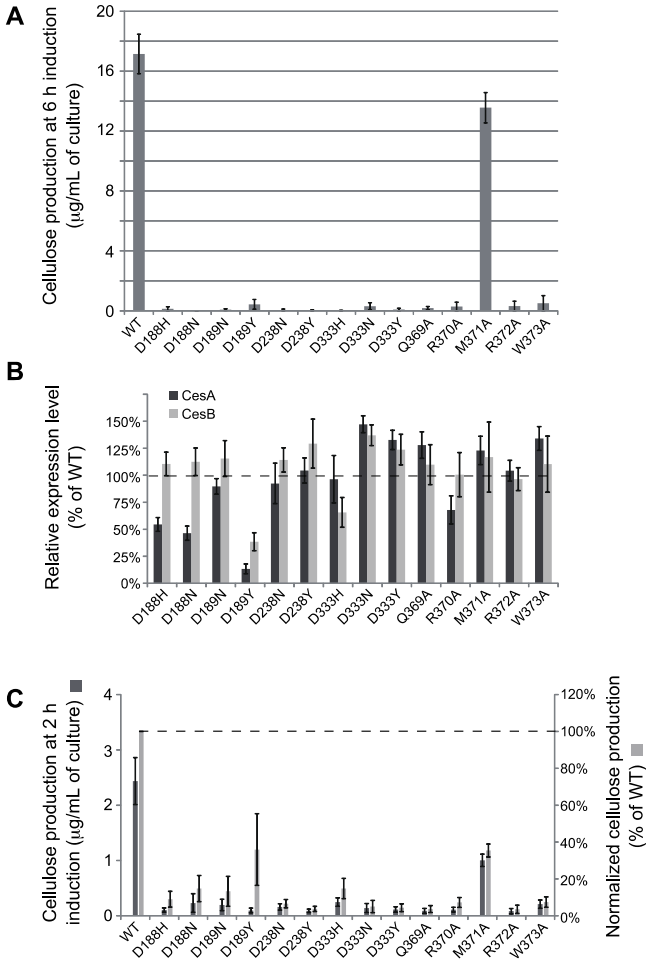

Figure 3.5 (A) Cellulose production at 6 h of induction (full yield) for wild type and point mutants in the D, D, D, QxxRW motif of GxCesA. Welch's *t*-test showed that all mutants produced significantly lower amounts of cellulose compared to the wild type enzyme ($P < 0.0001$), except the M371A mutant ($P = 0.066$). Cellulose produced by each mutant was determined at $n = 3$, while the determinations for the wild type enzyme were performed at $n = 7$. **(B)** Relative expression level of GxCesA and GxCesB at 2 h of induction. **(C)** Cellulose production at 2 h of induction. Light gray bars indicate the cellulose production yield normalized to CesA expression level, which is shown as the percentage of the wild type value. Error bars indicate the standard error of mean.

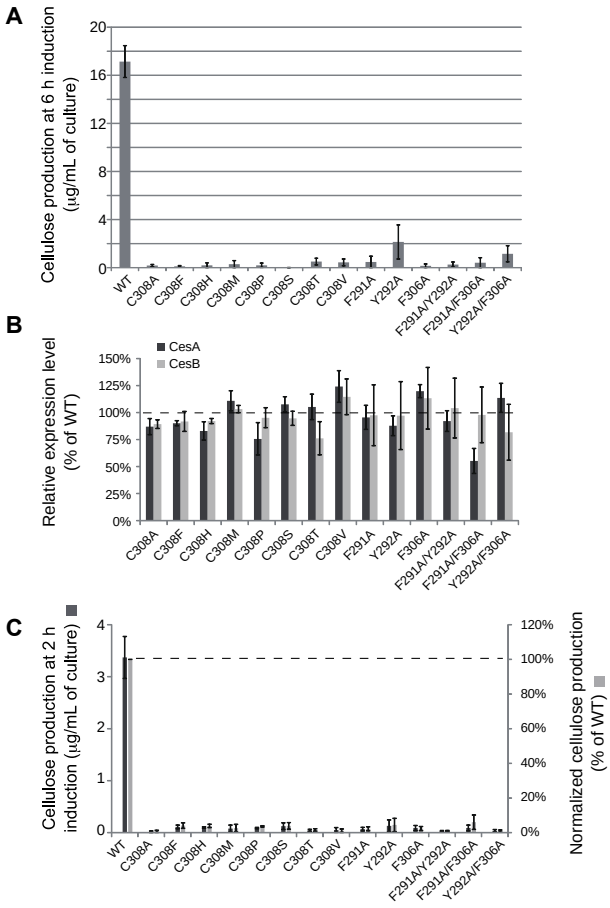

Figure 3.6 (A) Cellulose production at 6 h of induction (full yield) for the wild type enzyme, point mutants at C308 in the FFCGS motif, and mutations of aromatic residues around this motif (F291, Y292, and F306) to alanine. Welch's *t*-test showed that all mutants produced significantly lower amounts of cellulose compared to the wild type enzyme ($P < 0.0001$). The amount of cellulose produced by each enzyme was quantified at $n = 3$ or 5 (see Table 3.1), while the amount of cellulose produced by the wild type enzyme was quantified at $n = 7$. **(B)** The relative expression level of GxCesA and GxCesB at 2 h of induction. **(C)** Cellulose production at 2 h of induction. Light gray bars indicate the cellulose production yield of mutants normalized to CesA expression level, which are shown as a percentage of wild type. Error bars indicate the standard error of mean

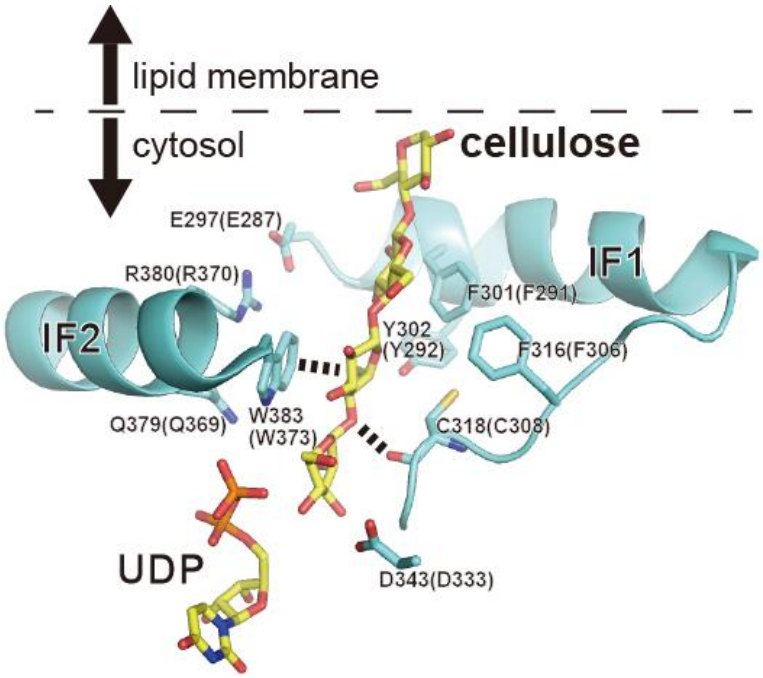

Figure 3.7 Close-up of the QxxRW and FFCGS motifs in the structural models of RsCesA in the c-di-GMP–free/UDP–bound state (PDB ID: 4HG6). The cellulose chain and UDP co-crystallized with RsCesA are shown in yellow, and RsCesA protein is shown in cyan. Amino acid numbering is based on the RsCesA protein. Black dashed lines indicate the interaction that Morgan (Morgan et al. 2013) proposed with their crystallographic analysis. The red dashed line indicates the sulfaur-arene interaction that we postulated based on our functional study and Morgan's structural analysis. Amino acid residues are numbered with the sequence of CesA protein of *R. sphaeroides* together with that of *G. xylinus* in parentheses, which was based on the alignment in Figure 3.3.

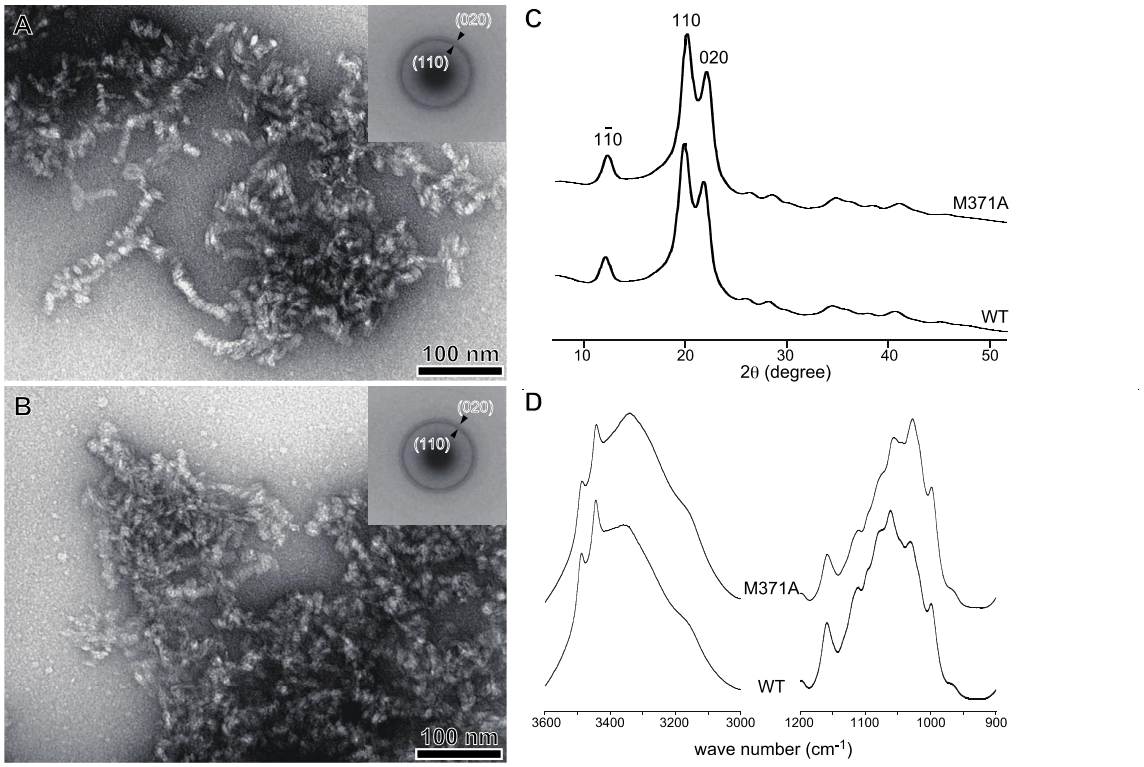

Figure 3.8 Structural analysis of cellulose produced by CESEC. **(A and B)** Electron micrographs of the washed product from WT (A) and GxCesA-M371A (B) by negative staining. Insets are electron diffraction diagrams taken from these washed samples: two diffraction rings are derived from the lattice of cellulose II crystal as shown (Langan P, et al. 2001). **(C)** Wide-angle X-ray diffraction profile of cellulose synthesized by recombinant GxCesAB protein with wild type and GxCesA M371A mutant. Major diffraction peaks are indexed by cellulose II as indicated. **(D)** FTIR spectra of cellulose synthesized by recombinant GxCesAB protein with wild type and M371A mutant of GxCesA.

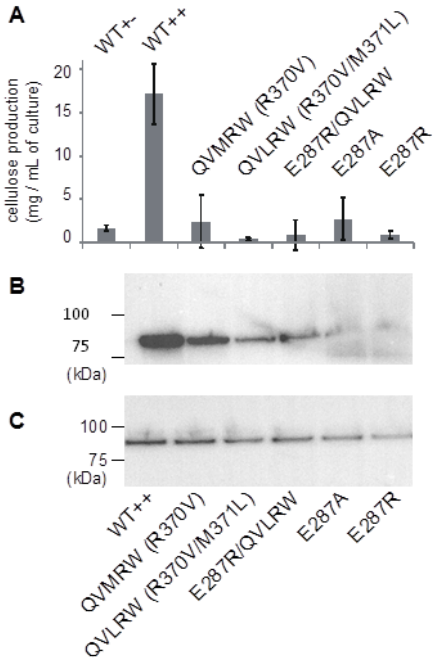

Figure 3.9 (**A**) Cellulose production by CESEC with wild type and point mutants plant-type sequence in the QxxRW motif. Negative and positive controls were the cellulose production by CESEC with wild type GxCesAB in which expression was induced by arabinose alone (WT+-), and arabinose plus IPTG (WT++), respectively. Error bars indicate the standard deviation. Welch's t-test showed that all mutants produced significantly lower amounts of cellulose as compared to the wild type enzyme (P <0.01). Cellulose produced by each enzyme was quantified at n =3, while that produced by the wild type enzyme was quantified at n =7. (**B and C**) Western blot analysis of the corresponding mutant proteins analyzed in panel A. Expression of GxCesA (**B**) and GxCesB (**C**) were analyzed using the *E. coli* cells after 2 h of induction.

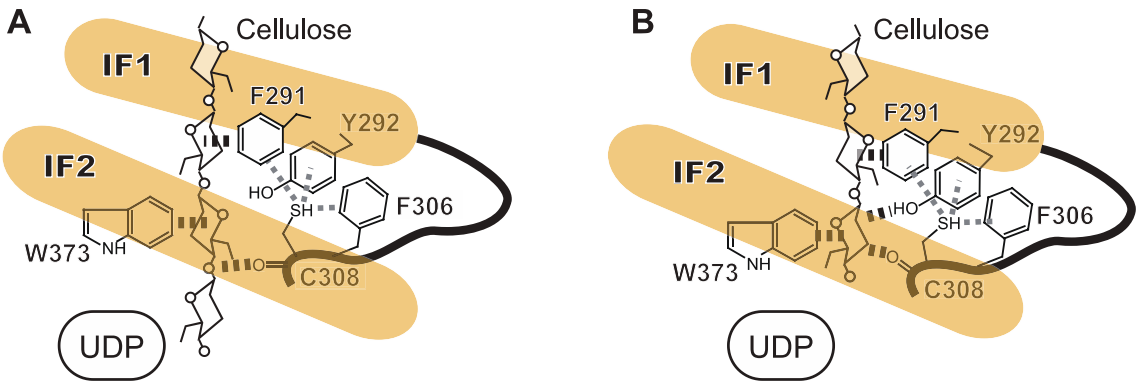

Figure 3.10 Schematic diagrams of the putative functional unit composed of the IF1 and IF2 helices and the FFCGS motif in bacterial CesA in two different states. The model in panel A is prepared from the PDB model 4HG6 (c-di-GMP–free and UDP–bound), while panel B is prepared from the PDB model 4P00 (c-di-GMP–bound and UDP–bound). Black and gray dashed lines indicate interactions in CesA proposed by the structural models (Morgan JLW et al. 2013; 2014) and this functional study (sulfur-arene interaction), respectively. Amino acid residues are numbered with the sequence of CesA protein of *G. xylinus* used in this study.

Table 3.1 Cellulose production by CESEC with mutant GxCesA proteins (6 h induction)

Mutation	Cellulose production by CESEC (μg/mL of culture; mean ±SEM [1])	*N*	Level of Significance [2]	
			from WT(++)	from WT(+-)
WT (+-; arabinose only) [3]	1.7 ± 0.21	3	*P* <0.0001	/
WT (++; arabinose and IPTG) [4]	0.30 ± 0.30	6	/	*P* <0.001
D188H	17 ± 1.3	3	*P* <0.0001	*P* =0.006
D188N	0.14 ± 0.14	3	*P* <0.0001	*P* =0.015
D189N	0.00 ± 0.00	3	*P* <0.0001	*P* =0.012
D189Y	0.08 ± 0.06	3	*P* <0.0001	*P* =0.042
D236N, D236H, D236Y	Failed to mutagenesis [5]	-	-	-
D238N	0.06 ± 0.06	3	*P* <0.0001	*P* =0.012
D238Y	0.03 ± 0.03	3	*P* <0.0001	*P* =0.014
D333H	0.02 ±0.02	3	*P* <0.0001	*P* =0.015
D333N	0.31 ± 0.23	3	*P* <0.0001	*P* =0.012
D333Y	0.09 ± 0.09	3	*P* <0.0001	*P* =0.009
Q369A	0.19 ± 0.10	3	*P* <0.0001	*P* =0.009
R370A	0.29 ± 0.29	3	*P* <0.0001	*P* =0.022
M371A	14 ± 1.0	3	*P* =0.066	*P* =0.005
R372A	0.32 ± 0.32	3	*P* <0.0001	*P* =0.031
W373A	0.51 ± 0.51	3	*P* <0.0001	*P* =0.136
C308A	0.18 ± 0.09	3	*P* <0.0001	*P* =0.010
C308F	0.12 ± 0.06	3	*P* <0.0001	*P* =0.012
C308H	0.20 ± 0.20	3	*P* <0.0001	*P* =0.007
C308M	0.29 ± 0.29	3	*P* <0.0001	*P* =0.023
C308P	0.20 ± 0.18	3	*P* <0.0001	*P* =0.006
C308S	0.51 ± 0.18	3	*P* <0.0001	*P* =0.015
C308T	0.51 ± 0.28	3	*P* <0.0001	*P* =0.033
C308V	0.44 ± 0.28	3	*P* <0.0001	*P* =0.028
F291A	0.48 ± 0.48	3	*P* <0.0001	*P* =0.113
Y292A	2.1 ± 1.4	5	*P* <0.0001	*P* =0.757
F306A	0.15 ± 0.15	3	*P* <0.0001	*P* =0.006
F291A/Y292A	0.26 ± 0.21	3	*P* <0.0001	*P* =0.009
F291A/F306A	0.41 ± 0.41	3	*P* <0.0001	*P* =0.074
Y292A/F306A	1.2 ± 0.67	3	*P* <0.0001	*P* =0.525

R370V	2.5 ± 3.1	3	P=0.0019	P=0.698
M371L	Failed to mutagenesis [5]	-	-	-
R370V/M371L	0.47 ± 0.15	3	P<0.0001	P=0.018
E287R/R370V/M371L	0.89 ± 1.8	3	P<0.0001	P=0.523
E287A	2.7 ± 2.4	3	P=0.00041	P=0.531
E287R	0.94± 0.42	3	P<0.0001	P=0.087

1 Standard error of mean.

2 Welch's *t*-test was conducted.

3 Cellulose synthesis in *E. coli* with L-arabinose induction to express diguanylate cyclase (c-di-GMP synthase) alone.

4 Cellulose synthesis in *E. coli* with L-arabinose and IPTG induction to express diguanylate cyclase and cellulose synthase, respectively.

5 We could not prepare the expression vector by either failures to ligate the mutated DNA fragment into an expression vector or site-directed mutagenesis itself on a sub-clonign vector.

Chapter 4 Visualization of cellulose synthase by immunofluorescence microscopy

4.1 Introduction

Cellulose is one of the major biopolymers on Earth. Despite its mass production on Earth by plants and other living organisms, destructive accumulation of cellulose on Earth has never been identified, although this has been observed for some synthetic plastics. This indicates that the cycle of synthesis and degradation shows a good balanced for cellulose on Earth, which is actually a striking feature of cellulose, suggesting it as a promising material for the sustainable human life.

All the cellulose on Earth is produced by living organisms, and originated from cellulose synthase complex (CSC) in the living cell (Somerville 2006). CSC is a hetero-subunit complex in the cell membrane. Electron microscopy of the freeze-fracture technique has been used to visualize CSC as a terminal complex (TC), which is a characteristic array of particles found on the cell membrane at the terminal of cellulose microfibril (Kimura et al. 1999; Kimura et al. 2001). Since 1970s, TCs has been found for many of the cellulose-producing organisms (a tunicate, alga, plants, and a bacterium) although the arrangement of the TC particles showed a variety of pattern (Itoh et al. 2007): linear type (for a bacterium, a tunicate, and alga producing a giant microfibril) and rosette-type (for higher plants and an algae from *Zygnematale*). Regardless of the specific pattern, such a regular array of cellulose-synthesizing enzyme

is considered to be important for cellulose microfibril formation by assembling many cellulose chains into a cellulose microfibril.

To date, several studies have identified the molecules included in CSC based on biochemical and molecular/cell biological analyses. For *Acetobacter* (now renamed for some strains as *Gluconacetobacter*, *Komagataeibacter*, and so on), a popular model for studying cellulose biosynthesis, six subunits are proposed to be included in CSC given the constitution of the genes related to cellulose synthesis (McNamara et al. 2015): GH-8 (also known as CMC – carboxymethyl cellulase) (Standal et al. 1994), ccp (cellulose complementing factor) (Standal et al. 1994), CesA, CesB, CesC, and CesD (Saxena et al. 1994; Wong et al. 1990). Among these, CesA is the catalytic subunit carrying the glycosyltransferase domain of the GT-2 family in the cytosolic part (Morgan et al. 2013), and CesA and CesB are the minimally required subunits for cellulose-synthesizing activity (Omadjela et al. 2013; Saxena et al. 1994; Wong et al. 1990). CesD is considered to control the crystallization process of cellulose microfibril (Hu et al. 2010; Saxena et al. 1994) and four chains are found inside the ring structure formed by the octamer of CesD protein (Hu et al. 2010). The functions of the other subunits have not yet clarified despite their clear relevance to the cellulose-synthesizing activity, as experimentally reported for GH-8 (Kawano et al. 2002; Kawano et al. 2008; Nakai et al. 2013), ccp2 (Sunagawa et al. 2013), CesC (Saxena et al. 1994), and CesD (Hu et al. 2010; Saxena et al. 1994; Sunagawa et al. 2013).

The SDS-freeze replica labeling (SDS-FRL) method (Fujimoto 1995), an immuno-labeling technique combined with freeze replica technique, is the direct methods to localize a specific protein in the TCs, and its application has shown that CesB protein is found in the linear TC of *Acetobacter* (Kimura et al. 2001). In addition,

fluorescence microscopy could also be used to successfully visualize the linear localization of GFP-fused CesD and ccp protein in the cell of *Acetobacter* (Sunagawa et al. 2013), which reminds that these two proteins are also included in the linear TCs of *Acetobacter*. These microscopic studies showed that CesB, CesD, and ccp protein form a part of the TC or the CSC of *Acetobacter*. However no report has provided concrete evidence that CesA protein is included in the linear TC of *Acetobacter*, although this is the widely accepted hypothesis given that CesA is the core subunit of the CSC. In the present study, CesA protein was successfully visualized as a linear array in the cell, and experimental evidence was obtained to show that CesA protein is included in the TC of *Acetobacter*.

4.2 Materials and Methods

4.2.1 Cell culture

Three different strains of *Acetobacter* were used in this study: ATCC53264, ATCC53524, and JCM9730. For convenience, the former name *Acetobacter* is used for these strains herein, although these are actually considered to be different species based on the current taxonomy (*Gluconacetobacter xylinus* for ATCC53264, *Komagataeibacter xylinus* for ATCC53524, and *Komagataeibacter sucrofermentans* for JCM9730). The two ATCC strains were provided by the American Type Culture Collection and the last strain was obtained from the Japan Collection Microorganisms at BRC-RIKEN, Japan. Each strain was grown in Schramm-Hestrin medium (Schramm and Hestrin 1954) at 30°C in a static condition for 3 to 5 days, until a sufficient amount of cellulose was produced. The cells were detached from the cellulose pellicle by shaking the culture medium and pressing the pellicle with a spatula, and then filtered by

37- or 50- μm pore-sized nylon mesh. The filtrated cells were collected by centrifugation (2000×*g* for 10 min at RT).

4.2.2 Antibody evaluation by western blot analysis

Western blot analysis was performed to evaluate whether the primary antibody has cross-reactivity with the proteins in the strains ATCC53264 and JCM9730, as well as strain ATCC53524 for which cross-reactivity has already been shown (Hashimoto et al. 2011). The primary antibodies used in this study were the same as those used in our previous studies (Hashimoto et al. 2011; Imai et al. 2014; Sun et al. 2016). In brief, each antibody is a polyclonal antibody against the synthetic peptide corresponding to a part of CesA (carboxyl terminal), CesB (a loop in the CBD2 domain), CesC (the part between the last six-TPR repeat and the carboxyl terminal region), and the CesD subunit (the loop between the β3 and β4 strands). The antigen peptide sequence for each of the proteins was designed from the sequence of the strain BPR2001 (Nakai et al. 1998) or JCM9730 (GenBank: AB010645) as reported in our previous study (Hashimoto et al. 2011). As shown in Table 4.1, high sequence similarity was found for each of the proteins between this strain and ATCC53264 or 1306-03 (GenBank: AAA21884-21887), and probably ATCC53524 or 1306-21, which is a derivative strain of ATCC53264 (Wong et al. 1990).

The centrifuged cells described above were resuspended in a buffer of 10 mM Tris-HCl (pH 8.0), 5 mM EDTA, 0.02% NaN_3, 50 μg/mL chloramphenicol. Then, the cell suspension was mixed with the SDS-PAGE sample buffer. After incubating at 4°C overnight, the sample was analyzed with a precast gel with a gradient of 5-20% acrylamide (SuperSep Ace, Wako Pure Chemicals Industries Ltd., Japan). The band

pattern was transferred from the gel to a PVDF membrane (Immobilon-P, Millipore Inc.), and then the membrane was incubated with each of the primary antibodies against CesA, CesB, CesC, and CesD protein. Finally, the protein band was visualized on the PVDF membrane by a chemical luminescence method with ECL select (GE Healthcare Inc.) and recorded by a CCD camera (EZ-capture, ATTO Inc., Japan).

4.2.3 Preparation of the cells for immunolabeling

The centrifuged cells were resuspended in CBS (citrate buffered saline: 50 mM sodium citrate buffer (pH 5.0), 136 mM NaCl, 2.7 mM KCl) and then incubated in 2% PFA (paraformaldehyde) in CBS at 4°C overnight to chemically fix the cells. Then, the gently centrifuged cells (1000×*g* for 10 min at RT) were resuspended in PBS (phosphate buffer saline: 10 mM phosphate buffer (pH7.4), 136 mM NaCl, 2.7 mM KCl) with 0.1 M glycine for quenching the PFA. The cell suspension was dropped on the glass coverslip, which was made to be hydrophilic in advance by dipping in 1 mg/mL poly-L-lysine solution at RT for 30 min. The coverslip carrying the cells was processed with the following procedures of lysozyme treatment and permeabilizing treatment, prior to the antibody treatment.

The cells on the coverslip were treated with 1 mg/mL lysozyme in TE buffer (100 mM Tris-HCl (pH 6.7), 5 mM EDTA) at 30°C for 1 h. After four repeated washes with PBS, the cells were permeabilized with 1% Nonidet P-40 in PBS at 30°C for 30 min. The cells were then washed four times with PBS for 5 min each time. Some of these treatments were skipped to explore the subunit localization in the cell.

4.2.4 Immunolabeling of the cells

Prior to the antibody treatment, the cells on the coverslip were incubated in 1% BSA and 1% blocking reagent (Roche Inc.) in PBS at RT for 1 h for blocking. Then, the cells were treated with the primary antibody solution, which was diluted 500-fold in blocking buffer, at 4°C overnight with gentle shaking. After four washes with PBS every 5 min, the cells were treated with 5 µg/mL of the fluorophore-conjugated anti-rabbit IgG (Alexa fluor 488, Life Technologies Inc.) in blocking buffer at RT for 2 h in the dark. The cells on the coverslip were washed with PBS four times every 5 min. The coverslip was taken out to wash the side without the cells in pure water, and then placed on the glass slide to seal the cells in the anti-fading reagent (SlowFade, Invitrogen Inc.).

The cells on the slide glass were observed on an IX71 microscope (Olympus Inc., Japan) with an oil immersion lens. Epi-fluorescence mode with a mercury lamp and the filter set FITC-2024B (Semrock Inc., USA) was used for recording the fluorescence image by a CCD camera (DP73, Olympus Inc., Japan). The same region of interest was also recorded with the phase contrast mode for subsequent merging with the fluorescence image.

4.2.5 SDS-freeze replica labeling

The cells collected from the pellicle as described above were quickly frozen on the gold sample career by dipping into liquid ethane at −175°C with a Leichert KF-80 system (Leica Inc.). The freeze-fracture replica of these cells without chemical fixation was prepared using a BAF-400D system (Balzers Inc.). The fracture was performed at −113°C, and then platinum/carbon was evaporated on the fractured surface at an angle of 45° followed by rotary carbon coating to support the platinum replica. The prepared replica was treated in the lysozyme solution (1 mg/mL lysozyme in 25 mM Tris-HCl

(pH 8.0), 10 mM EDTA) for 4 h at RT, and subsequently in the lysis solution (2.5% SDS, 10 mM Tris-HCl (pH 8.0)) for 2 h at RT. After washing three times with PBS, the replica was then incubated in the blocking solution (1% BSA in PBS) for 30 min at RT, and then treated with the primary antibody diluted in the blocking buffer overnight at 4°C. The replica was then washed in PBS with 0.05% Tween-20 (PBST) and treated with the secondary antibody (anti-rabbit IgG conjugated with 15-nm colloidal gold, British BioCell International, UK) for 1.5 h at RT. Finally, the replica was treated with 0.5% glutaraldehyde in PBS for 15 min at RT, and then transferred on the carbon-coated copper grid after washing with water.

The replica on the grid was observed by a JEM-2000EXII (Jeol Inc., Japan) electron microscope and the images were recorded with photo-emulsion (FG film, FujiFilm Inc., Japan), which was developed by Korectol (FujiFilm Inc., Japan) for 4 min at 20°C.

4.3 Results

4.3.1 CesA is present in the linear array in the bacterial cells

The results of the western blot analysis with the antibodies used in this study are shown in Figure 4.1. These antibodies basically showed cross-reactivity to the proteins extracted from *Acetobacter* in the three different strains used in this study (ATCC 53524, ATCC53264, and JCM9730). We then used these antibodies for immunolabeling fluorescence microscopy, as shown in Figure 4.2.

As a result of optimizing the pretreatment of the cells (fixation, lysozyme treatment, and detergent treatment) as well as the antibody treatment, we could successfully label CesA and CesD proteins as a linear array in the cell (Figure 4.2) whereas such a linear labeling pattern was not found for the immunolabeling of CesB and CesC (Figure 4.3).

CesB labeling only could be visualized in the top of few cells while CesC labeling was found in the whole cells of most cells by using strain ATCC 53524. The linear labeling pattern of CesA and CesD was observed for all of the strains used in this study. This clearly indicates that CesA and CesD proteins are the subunits included in the linear TC of *Acetobacter*. Furthermore the linear signal was sometimes found at the lateral edge of the cell on the micrograph, indicating that the labeled protein is not on the inside but rather at the boundary of the *Acetobacter* cell. Therefore, the linear immunolabeling pattern shown in Figure 4.2 provides the experimental evidence that CesA and CesD are included in the linear TC on the cell membrane, the bacterial CSC.

4.3.2 Change of the immunolabeling efficiency for CesA and CesD protein.

For efficient immunolabeling, the cells are usually treated with an adequate procedure prior to labeling. In the case of the bacterial cell, lysozyme treatment is commonly used for damaging the outer membrane by disintegrating the peptidoglycan layer, and detergent treatment is used for permeabilizing the inner membrane. Therefore, in principle, the protein exposed to the outside of the cell will be labeled without any pretreatment. We then surveyed the change in the immunolabeling efficiency depending on the pretreatment applied to explore the location of CesA and CesD proteins, which were successfully immunolabeled in this study. The strain ATCC53524 was used for this purpose given the fact that this strain showed the highest immunolabeling efficiency.

We tested five different pretreatments, in addition to the optimized condition shown above (Figures 4.4A and 4.5A): (i) no treatments, (ii) EDTA treatment, (iii) detergent treatment, (iv) EDTA treatment followed by detergent treatment, and (v) lysozyme

treatment (Figures 4.4 and 4.5, and summarized in Table 4.2). First, the cells with no pretreatment showed almost no immunolabeling for neither CesA nor CesD (Figures 4.4B and 4.5B), indicating that CesA and CesD are not exposed to the outside of the cell. Notably, EDTA treatment alone allowed for the immunolabeling of CesD but not CesA (Figures 4.4C and 4.5C). Given the relatively mild disturbance of the outer membrane only by depletion of divalent cations with EDTA, CesD is probably located in the periplasmic space and was immunolabeled due to access of the antibody. By contrast, CesA protein is a transmembrane protein, with its carboxyl terminal (the epitope of the antibody used in this study) facing to the cytoplasm. Therefore, it is reasonable that CesA was not immunolabeled for cells whose outer membrane is mildly disturbed by EDTA alone, which is not harsh enough to allow for cell lysis.

Detergent treatment alone did not allow for the immunolabeling of CesA and CesD, in contrast to the expectation (Figures 4.4D and 4.5D). However, EDTA treatment prior to detergent treatment dramatically improved the immunolabeling efficiency for both CesA and CesD (Figures 4.4E and 4.5E). This indicates that the permeabilization by the detergent is not sufficient for disturbing the outer membrane of *Acetobacter* to introduce the antibody to the inside of the cell (periplasm and cytoplasm).

A substantial number of cells were immunolabeled when treated with lysozyme alone for both CesA and CesD (Figures 4.4F and 4.5F). Given that CesD is localized in the periplasm, as shown above, the lysozyme treatment without permeabilizing the inner membrane was sufficient to immunolabel CesD protein. However the substantial immunolabeling of CesA protein from such pretreatment requires a speculative interpretation given that the carboxyl terminal of CesA protein (the epitope of the antibody used in this study) is on the cytoplasmic side and prevents access of the

antibody unless the inner membrane is permeabilized. We consider that this observation reflects weak but nevertheless significant cell lysis due to the lysozyme treatment.

4.4 Discussions

4.4.1 Relationship between cellulose synthase A and D in *Gluconacetobacter xylinus* cell wall

This study provides evidence that CesA is included in the TC of bacterial cells, which had already been reported for plant cells (Kimura et al. 1999). Based on fluorescence immuno-microscopy, this study also showed that CesD is included in the linear TC, as reported previously (Sunagawa et al. 2013). These observations are not sufficient to conclude that the CesA and CesD proteins are colocalized in the TC. Direct immunolabeling with a fluorescence dye-labeled primary antibody should provide a clearer conclusion for the colocalization of CesA and CesD proteins in the TC. Neverthelss, the linear labeling pattern observed for CesA and CesD in this study is striking enough to propose that CesA and CesD are colocalized in the TC of *Acetobacter*, regardless of whether their interaction is direct or indirect.

The structural models for the CesA/CesB complex (Morgan et al. 2016; Morgan et al. 2013; Morgan et al. 2014) and CesD (Hu et al. 2010) also support the functional link between CesA and CesD, given that the former generates cellulose from UDP-glucose and the latter includes cellulose chains in the channel formed by its homo-octamer. It is then proposed that CesD functions downstream of the CesA/CesB complex in the process of cellulose biosynthesis, and that they are spatially close. This hypothesis is

consistent with the observation that immunolabeling of CesA and CesD proteins showed a linear pattern in the cells in this study.

4.4.2 Why CesB and CesC cannot be linearly labeled?

We also attempted the immunolabeling of CesB and CesC protein in this study although no successful data were obtained. For CesC protein, which is currently the most enigmatic subunit, the reason for the failure is unclear. A possible reason could be related to access of the antibody to the epitope, which is significantly influenced by the stereo arrangement of this subunit in the cell. However, it was unexpected that the immunolabeling of CesB protein did not show a linear labeling pattern as observed by SDS-FRL in a previous study (Kimura et al. 2001). Given that the antibody against CesB used for fluorescence immunolabeling in this study allowed for the linear TC to be labeled by SDS-FRL (Figure 4.6), this antibody should also be able to label the SDS-treated freeze-replica prepared from the unfixed cells. Therefore, a possible interpretation for this unexpected result is that the PFA fixation might kill the epitope activity of the protein, for example by changing the CesB protein itself and/or its surrounding environment, so as to inhibit access of the antibody.

4.4.3 Toward further understands 3D model of cellulose synthase

Compiling the results of this and previous studies, we propose a hypothetical model for the TC of *Acetobacter* as shown in Figure 4.7. The CesA/CesB complex is embedded in the inner membrane, given that the ligands (UDP-glucose and c-di-GMP) are cytosolic molecules and the product cellulose is extruded outside through the membrane-spanning channel (Morgan et al. 2013). CesC is depicted as the cellulose-translocating channel in the outer membrane according to the currently

accepted model (McNamara et al. 2015, Saxena et al. 1994). No immunolabeling from the lack of pretreatment, and weak immunolabeling from EDTA treatment alone for CesD protein indicated that CesD is located in the periplasmic space. The results of a biochemical study using marker enzyme assays also support this hypothesis (Iyer et al. 2011). Given that the function of CesD is carried out downstream of CesA as discussed above, CesD protein is located close to the exit of the cellulose-translocation channel of CesA protein in the periplasm, as proposed based on a previous structural analysis of the *Acetobacter* CesA/CesB complex with electron microscopy (Du et al. 2016).

Given that one CesA/CesB complex produces one cellulose chain (Morgan et al. 2013), and the CesD oligomer includes four chains in its inner pore (Hu et al. 2010), the model in Figure 4.7a represents only one CesA/CesB complex, and the other three complexes are not shown for visual clarity. A combination of these molecules could be the functional unit to produce the primary assembly of the polymerized cellulose chains prior to microfibril formation, which has been proposed as a "mini-sheet" in a previous study (Cousins and Brown 1995). The linear array of this whole complex should be visualized as the linear type TC in *Acetobacter* (Figure 4.7b).

The SDS-FRL experiment also provided insight about CesB protein. Given the smoothness of the fractured surface, the linear TC of *Acetobacter* is found in the P-face (the extracellular surface of the inner leaflet of the lipid bilayer) of the outer membrane (Kimura et al. 2001). The successful immunolabeling of CesB protein by SDS-FRL indicates that this protein remains with the replica even after SDS-treatment, indicating that CesB protein significantly interacts with the outer membrane from the periplasmic side. This interaction is likely important for guiding the cellulose chain to the

extracellular side and/or the crystallization of cellulose chains into a microfibril. Further SDS-FRL experiment with other antibodies will shed light on the locations of the other subunits.

4.5 Summaries

This study demonstrated that CesA, the core catalytic subunit of cellulose synthase, is the molecule included in the linear-type TC or the CSC of *Acetobacter*. Structural analysis of these proteins has recently started providing many insights about the enzymatic mechanism of cellulose synthase as well as other well-known membrane proteins such as ion/water channels and transporters. However, for cellulose synthase, which functions in the assembly of polymer chains into a super molecular aggregation, the structural analysis of the protein complex at a cellular/subcellular scale is important for understanding the underlying mechanism. Further studies with microscopy will play an important role for shedding light on the mechanism of cellulose chains assembly into the microfibril.

FIGURE CAPTIONS

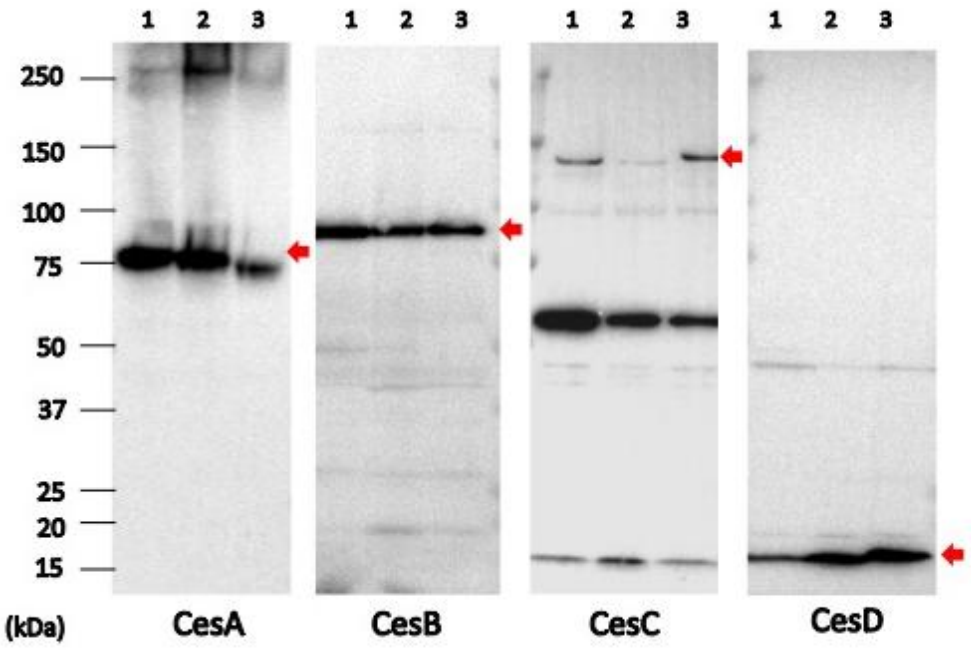

Figure 4.1 Western blot analysis with SDS-PAGE for the whole cell sample of *Acetobacter* cells. A, B, C, and D show the results with the antibody against CesA, CesB, CesC, and CesD protein, respectively. The sample of ATCC53524, ATCC53264, and JCM9730 was loaded into the lane 1, 2, and 3, respectively. Roughly the same number of cells, measured by the optical density at 600 nm, were loaded. The arrow indicates the band of interest.

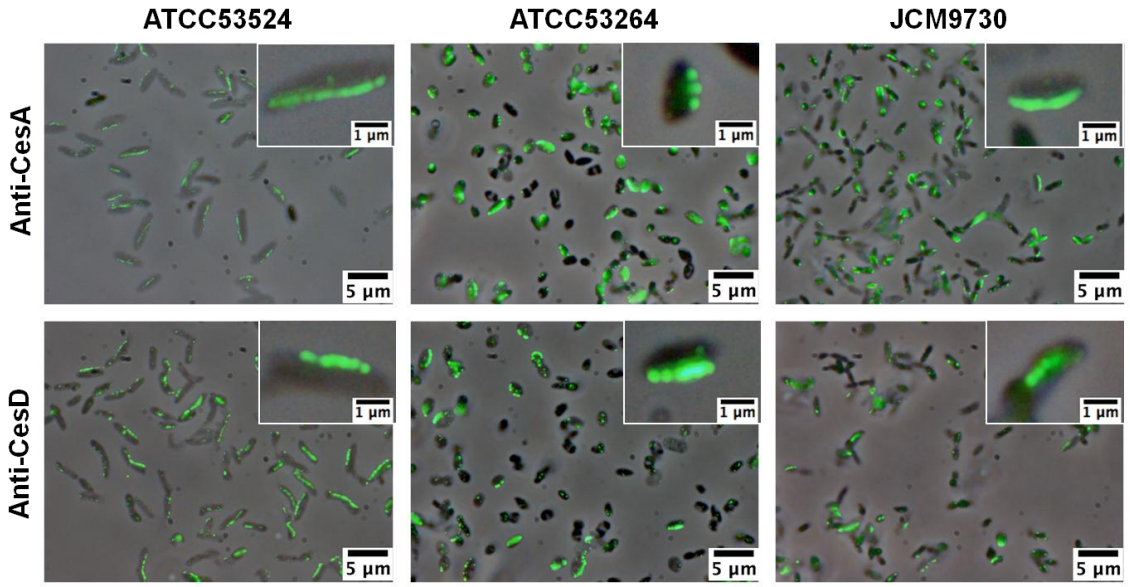

Figure 4.2 Fluorescence micrographs of lysozyme and detergent pretreated *Acetobacter* cells with immunolabeling by the antibodies against CesA and CesD proteins. Three different strains (ATCC53524, ATCC53264, and JCM9730) were labeled using the identical protocol. The phase-contrast images and the epi-fluorescence image are merged. The inset shows the image at a higher magnification.

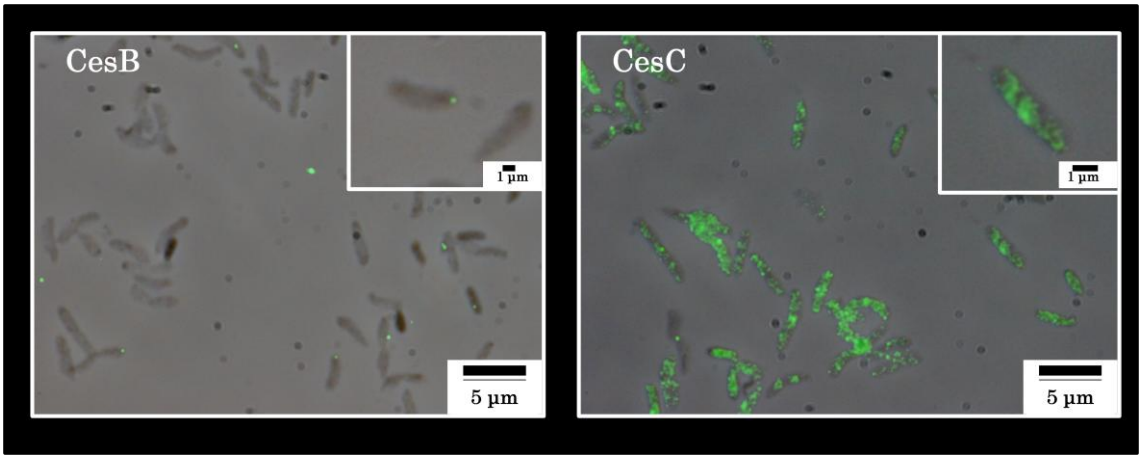

Figure 4.3 Fluorescence micrographs with immunolabeling of the strain ATCC53524 by the antibody against CesB and CesC proteins, merged on the phase-contrast image. The inset shows the image at a higher magnification.

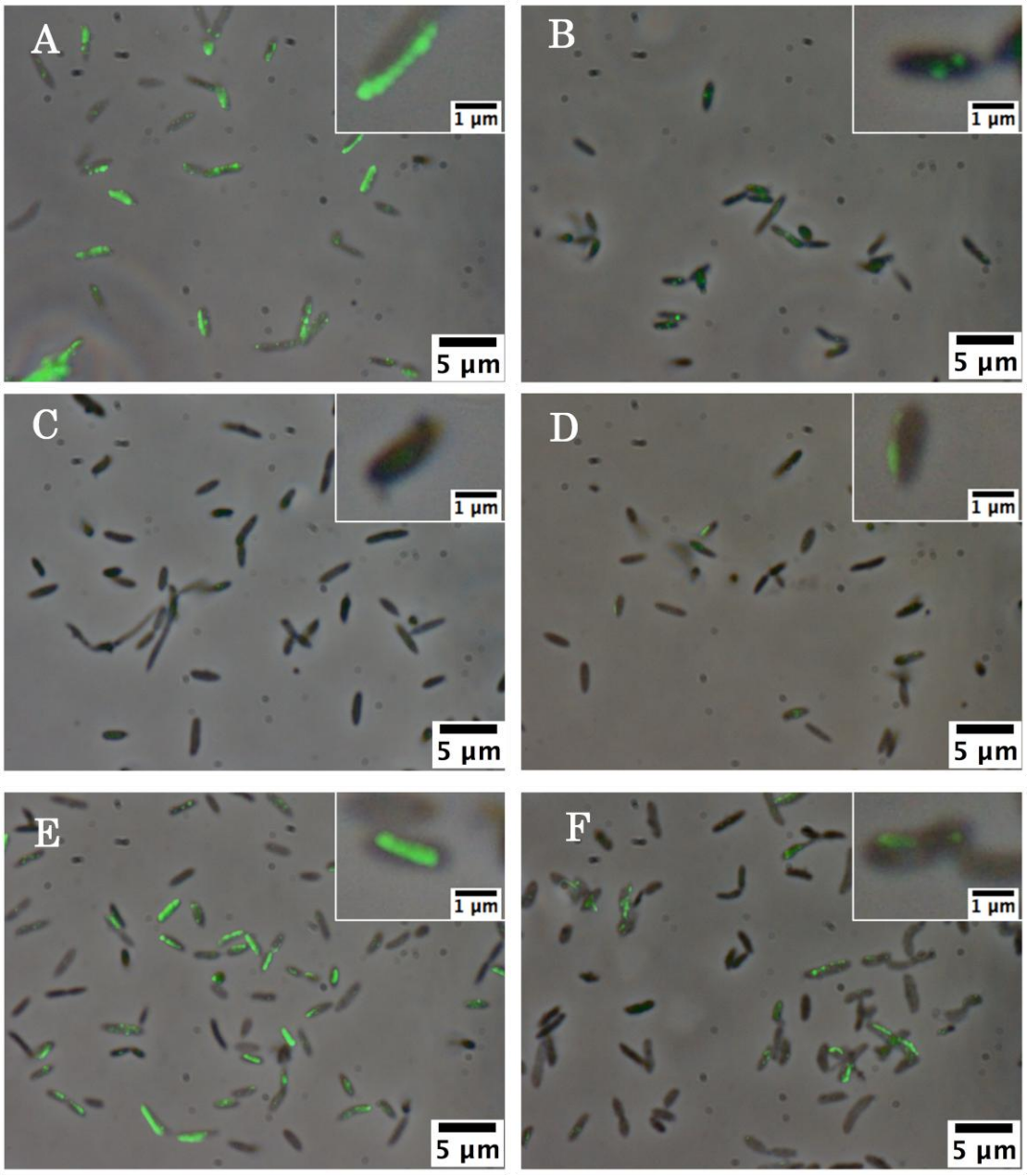

Figure 4.4 Fluorescence micrographs with immunolabeling of the strain ATCC53524 by the antibody against CesA protein, merged on the phase-contrast image. Pretreatment of the cell prior to the primary antibody treatment was as follows: (A) lysozyme treatment followed by detergent treatment (the optimized condition in this study), (B) no pretreatment, (C) EDTA treatment, (D) detergent treatment, (E) EDTA treatment followed by detergent treatment, (F) lysozyme treatment. The inset shows the image at a higher magnification.

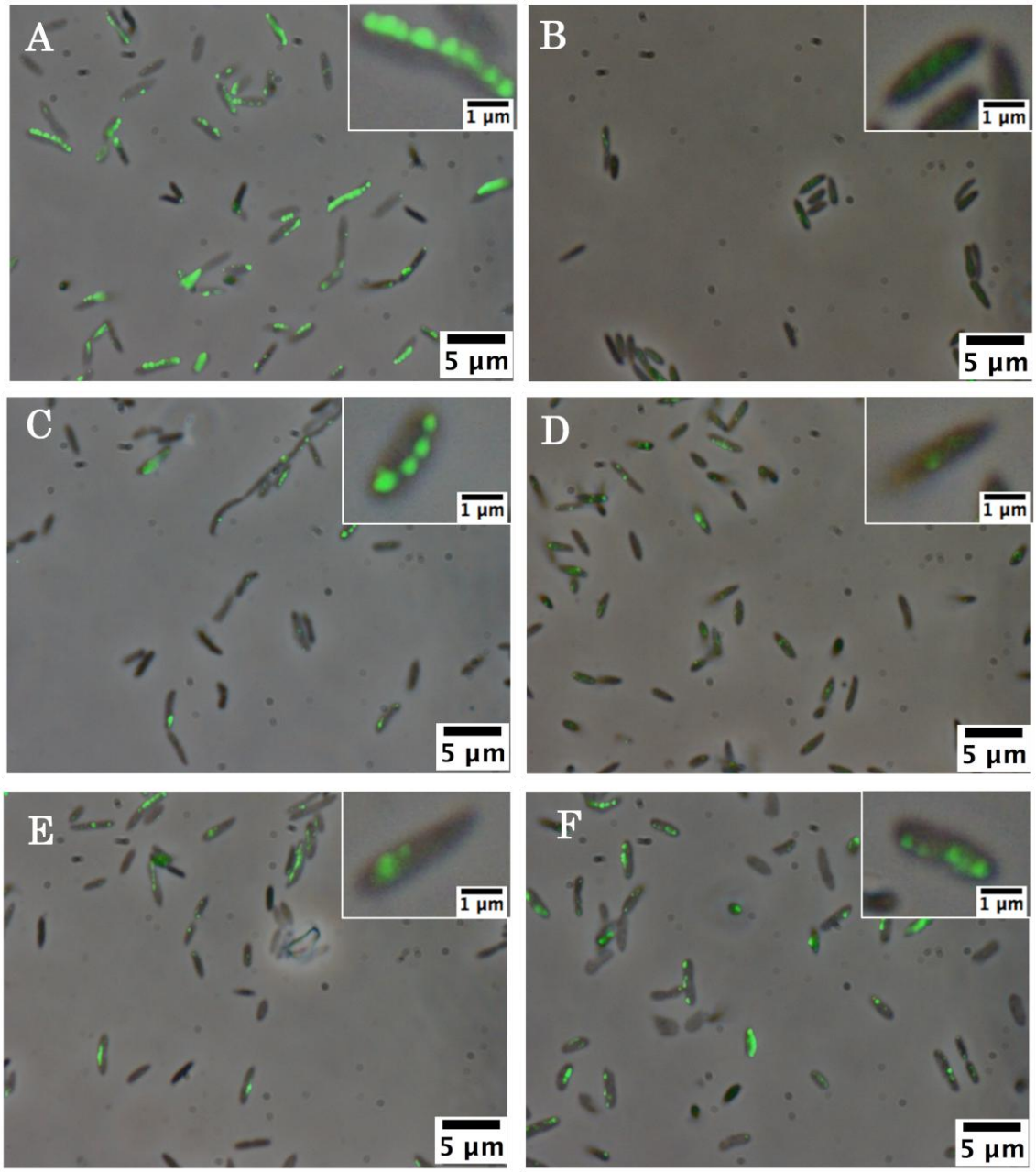

Figure 4.5 Fluorescence micrographs with immunolabeling of the strain ATCC53524 by the antibody against CesD protein, merged on the phase-contrast image. Pretreatment of the cell prior to the primary antibody treatment was as follows: (A) lysozyme treatment followed by detergent treatment (the optimized condition in this study), (B) no pretreatment, (C) EDTA treatment, (D) detergent treatment, (E) EDTA treatment followed by detergent treatment, (F) lysozyme treatment. The inset shows the image at a higher magnification.

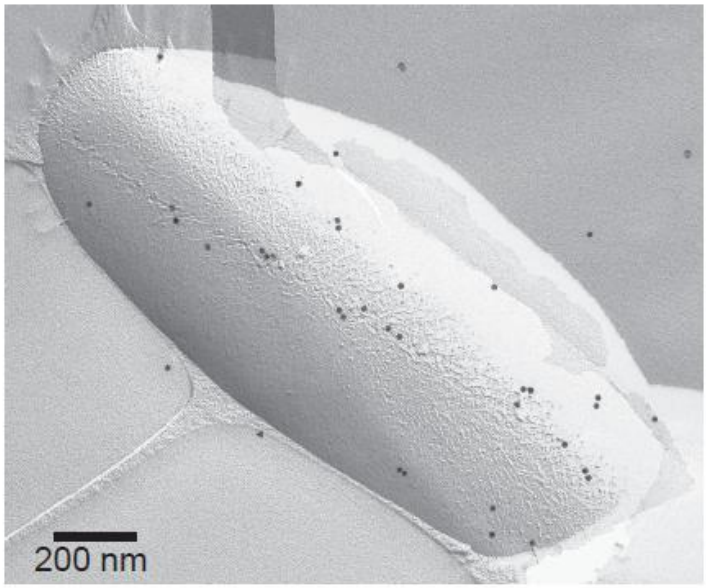

Figure 4.6 Electron micrograph of SDS-FRL for the strain ATCC53524 with the antibody against CesB protein. The antibody location was visualized by colloidal gold of a 15 nm diameter.

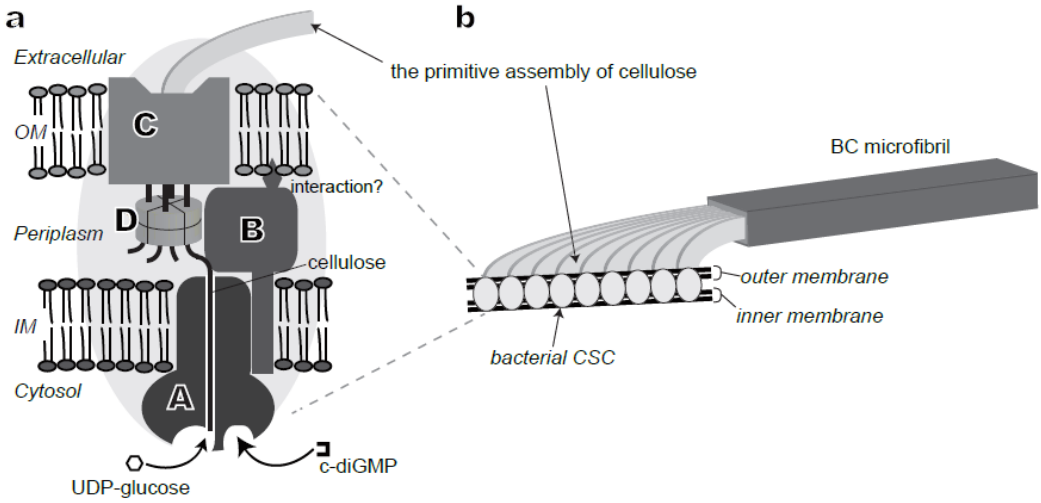

Figure 4.7 A schematic model for the cellulose synthase complex of *Acetobacter*. In the schematic diagram of the subunit location in one complex (a), CesA and CesB are depicted as monomers while CesD is illustrated as an octamer through which four cellulose chains pass, as reported previously (Hu et al. 2010). CesC is located in the outer membrane according to the currently accepted model (McNamara et al. 2015; Saxena et al.1994). The terminal complexes are probably formed by the linear array of these complexes as shown in (b). OM: outer membrane; IM: inner membrane

Table 4.1 Amino acid sequences of the peptide antigens for the antibodies used in this study (JCM9730), together with the sequence of the corresponding part for ATCC53264. The non-identical residues are indicated with shadowing.

Protein and strain		Amino acid sequence
CesA	JCM9730 (antigen)	S G Q T Q E G K I S R A A S
	ATCC53264	S G Q T Q E G K I S R A A S
CesB	JCM9730 (antigen)	S P D L Y T W R D R P N K
	ATCC53264	S P D L Y T W R D R P Y K
CesC	JCM9730 (antigen)	P S I D G G L G F R S R S G E H
	ATCC53264	P S I D G G L G F R S R S G E H
CesD	JCM9730 (antigen)	T R D I D A E D L N S
	ATCC53264	T R D I D A E D L N S

Table 4.2 Summary of the immunolabeling microscopy observations

Pre-treatment after PFA fixation	CesA	CesD
Lysozyme treatment + Detergent treatment	+++	+++
No treatment	−	−
TE* treatment	−	+
Detergent treatment	−	−
TE treatment + Detergent treatment	++	++
Lysozyme treatment	++	++

−: Almost no labeling was found

+: A small number of the cells were labeled

++: A substantial number of the cells were labeled

+++: Most of the cells were labeled

*: Tris-EDTA buffer (100 mM Tris-HCl (pH 6.7), 5 mM EDTA), the same buffer used for the lysozyme treatment

Chapter 5 Conclusions and future directions

This thesis aimed for understanding the process of cellulose biosynthesis. By establishing an easy cellulose functional analysis system, the aim was achieved partially. The results of each chapter are summarized as follows:

In Chapter 2, cellulose-synthesizing activity is successfully reconstituted in *E. coli* by expressing the bacterial cellulose synthase complex of *Acetobacter xylinus*: CesA and CesB. Cellulose synthase activity was, however, only detected when CesA and CesB were coexpressed with diguanyl cyclase (DGC), which synthesizes cyclic-di-GMP (c-di-GMP), activity in bacteria. Direct observation by electron microscopy revealed extremely thin fibrillar structures outside *E. coli* cells, which were removed by cellulase treatment. This fiber structure is not likely to be the native crystallographic form of cellulose I, given that it was converted to cellulose II by a chemical treatment milder than ever described. We thus putatively conclude that this fine fiber is an unprecedented structure of cellulose. Despite the inability of the recombinant enzyme to synthesize the native structure of cellulose, the system described in this study, named "CESEC (CEllulose-Synthesizing *E. Coli*)", represents a useful tool for functional analyses of cellulose synthase and for seeding new nanomaterials.

In Chapter 3, we conducted a functional analysis of cellulose synthase with site-directed mutagenesis, by using recombinant cellulose synthase reconstituted in living CESEC. We demonstrated that inactivating mutations at an important amino acid residue reduced cellulose production. An interesting loss-of-function mutation occurred

on Cys308, whose main chain carbonyl plays an important role for locating the cellulose terminus. Mutating this cysteine to serine, thus changing sulfur to oxygen in the side chain, abolished cellulose production in addition to other apparent detrimental mutations. This unexpected result highlights that the thiol side-chain of this cysteine plays an active role in catalysis, and additional mutation experiments indicated that the sulfur–arene interaction around Cys308 is a key in cellulose-synthesizing activity. Data obtained by CESEC shed light on the function of cellulose synthase in living cells, and will deepen our understanding of the mechanism of cellulose synthase.

In Chapter 4, fluorescence immuno-microscopy is used to show that CesA protein, the catalytic subunit, is included in the terminal complex of *Acetobacter*. Furthermore, we discuss the obtained microscopic data for improving our understanding of the molecular organization in the bacterial cellulose synthase complex. Further studies with microscopy will play an important role for shedding light on the mechanism of cellulose chains assembly into the microfibril.

In conclusion, cellulose synthase was functional reconstitute in *E.coli* and named CESEC. The function of CesA could be analysis. Even the product produced by CESEC is not cellulose I but cellulose II. Moreover, CesC, CesD, CMCax or ccp could be reconstituted into *E.coli* for the functional analysis of cellulose synthase. Furthermore, the localization of cellulose synthase could be analyzed by immuno-microscopy. These developments of biosynthesis gave the basic information for further understanding the function of cellulose synthase and will direct the utilized of cellulose.

References

Aloni Y, Delmer DP, Benziman M (1982) Achievement of high rates of in vitro synthesis of β1→4-glucan: Activation by cooperative interaction of the *Acetobacter xylinum* enzyme system with GTP, polyethylene glycol, and a protein factor. Proc Natl Acad Sci USA 79: 6448-6452

Amikam D, Galperin MY (2006) PilZ domain is part of the bacterial c-di-GMP binding protein. Bioinformatics 22:3-6

Andress KR (1929) The X-ray diagram of mercerized cellulose. Zietschrift Physikalische Chemie Abstracts B 4, 190-206.

Atalla RH, VanderHart DL (1984) Native cellulose: A composite of two distinct crystalline forms. Science 223:283-285

Baba T, Ara T, Hasegawa M, Takai Y, Okumura Y, Baba M, Datsenko KA, Tomita M, Wanner BL, Mori H (2006) Construction of Escherichia coli K-12 in-frame, single-gene knockout mutants: The Keio collection. Mol Sys Biol 2:1-13

Brown Jr. RM (1996) The biosynthesis of cellulose. J Macromol Sci- Pure Appl Chem 33:1345-1373

Brummell DA, Catala C, Lashbrook CC, Bennett AB (1997) A membrane-anchored E-type endo-1,4-β-glucanase is localized on Golgi and plasma membranes of higher plants. Proc.Natl. Acad. Sci. USA 94:4794-99

Buleon A, Chanzy H, Roche E (1977) Shish Kebab-like structures of cellulose. J Polym Sci Part B Polym Lett 15:265-270

Bureau TE, Brown Jr. RM (1987) In vitro synthesis of cellulose II from a cytoplasmic membrane fraction of *Acetobacter xylinum*. Proc Natl Acad Sci U S A 84:6985-6989

Christen M, Christen B, Allan MG, Folcher M, Jenö P, Grzesiek S, Jenal U (2007) DgrA is a member of a new family of cyclic diguanosine monophosphate receptors

and controls flagellar motor function in Caulobacter crescentus. Proc Natl Acad Sci U S A 104:4112-4117

Chu Z, Chen H, Zhang Y, Zhang Z, Zheng N, Yin B, Yan H, Zhu L, Zhao X, Yuan M, Zhang X, Xie Q (2007) Knockout of the AtCESA2 gene affects microtubule orientation and causes abnormal cell expansion in Arabidopsis. Plant Physiol 143:213-224

Colombani A, Djerbi S, Bessueille L, Kristina B, Ohlsson A, Berglund T, Teeri TT, Bulone V (2004) In vitro synthesis of (1→3)-β-D-glucan (callose) and cellulose by detergent extracts of membranes from cell suspension cultures of hybrid aspen. Cellulose 11:313-327

Cousins SK, Brown Jr. RM (1995) Cellulose I microfibril assembly: computational molecular mechanics energy analysis favours bonding by van der Waals forces as the initial step in crystallization. Polymer 36:3885-3888

Czaja W, Krystynowicz A, Bielecki S, Brown Jr. RM (2006) Microbial cellulose - the natural power to heal wounds. Biomaterials 27:145-151

Delmer DP (1999) Cellulose biosynthesis: Exciting times for a difficult field of study. Annual Review of Plant Biology 50:245-276

Delmer DP, Benziman M, Padan E (1982) Requirement for a membrane potential for cellulose synthesis in intact cells of *Acetobacter xylinum*, Proc Natl Acad Sci U S A 79:5282-5286

Dorfmueller HC, Ferenbach AT, Borodkin VS, Van Aalten DMF (2014) A structural and biochemical model of processive chitin synthesis. J Biol Chem 289:23020-23028

Draper, O. Byrne ME, Li Z, Keyhani S, Barrozo JC, Jensen G, Komeili A (2011) MamK, a bacterial actin, forms dynamic filaments in vivo that are regulated by the acidic proteins MamJ and Lim. J Mol Microbiol 82:342-354

Du J, Vepachedu V, Cho SH, Kumar M, Nixon BT (2016) Structure of the cellulose synthase complex of *Gluconacetobacter hansenii* at 23.4 Å resolution. PLoS ONE 11. doi: 10.1371/journal.pone.0155886

Duan G, Smith VH, Weaver DF (2001) Characterization of aromatic-thiol π-type hydrogen bonding and phenylalanine-cysteine side chain interactions through ab

initio calculations and protein database analyses. Mol. Physics 99:1689-1699

Endler A, Sánchez-Rodríguez C, Persson S (2010) Glycobiology: Cellulose squeezes through. Nature Chemical Biology 6:883-884

Fisher D, Cyr R (1998) Extending the microtubule/microfibril paradigm. Cellulose synthesis is required for normal cortical microtubule alignment in elongating cells. Plant Physiol 116:1043-1051

Frankel RB, Bazylinski DA (2006) How magnetotactic bacteria make magnetosomes queue up. Trends Microbiol 14: 329-331

Fujii S, Hayashi T, Mizuno K (2010) Sucrose synthase is an integral component of the cellulose synthesis machinery. Plant and Cell Physiology 51:294-301

Fujimoto K (1995) Freeze-fracture replica electron microscopy combined with SDS digestion for cytochemical labeling of integral membrane proteins -Application to the immunogold labeling of intercellular junctional complexes. J Cell Sci 108:3443-3449

Gu Y, Kaplinsky N, Bringmann M, Cobb A, Carroll A, Sam-pathkumar A, Baskin TI, Persson S, Somerville CR (2010) Identification of a cellulose synthase-associated protein required for cellulose biosynthesis. Proc Natl Acad Sci U S A 107:12866-12871

Guerriero G, Fugelstad J, Bulone V (2010) What do we really know about cellulose biosynthesis in higher plants? Journal of Integrative Plant Biology 52:161-175

Guzman LM, Belin D, Carson MJ, Beckwith J (1995) Tight regulation, modulation, and high-level expression by vectors containing the arabinose PBAD promoter. J Bacteriol 177:4121-4130

Hashimoto A, Shimono K, Horikawa Y, Ichikawa T, Wada M, Imai T, Sugiyama J (2011) Extraction of cellulose-synthesizing activity of *Gluconacetobacter xylinus* by alkylmaltoside. Carbohydr Res 346:2760-2768

Hayashi N, Sugiyama J, Okano T, Ishihara M (1997) Selective degradation of the cellulose I(α) component in Cladophora cellulose with Trichoderma viride cellulase. Carbohydr Res 305:109-116

Hayashi N, Sugiyama J, Okano T, Ishihara M. (1998) The enzymatic susceptibility of cellulose microfibrils of the algal-bacterial type and the cotton-ramie type. Carbohydr Res 305:261-269

Hiraishi M, Igarashi K, Kimura S, Wada M, Kitaoka M, Samejima M (2009) Synthesis of highly ordered cellulose II in vitro using cellodextrin phosphorylase. Carbohydr Res 344:2468-2473

His I, Driouich A, Nicol F, Jauneau A, Hofte H (2001) Altered pectin composition in primary cell walls of korrigan, a dwarf mutant of Arabidopsis deficient in a membrane-bound endo-1,4-β-glucanase. Planta 212:348-58

Holland N, Holland D, Helentjaris T, Dhugga KS, Xoconostle-Cazares B, Delmer DP (2000) A comparative analysis of the plant cellulose synthase (Cesa) gene family. Plant Physiol 123:1313-1323

Hu S-Q, Gao Y-G, Tajima K, Sunagawa N, Zhou Y, Kawano S, Fujiwara T, Yoda T, Shimura D, Satoh Y, Munekata M, Tanaka I, Yao M (2010) Structure of bacterial cellulose synthase subunit D octamer with four inner passageways. Proc Natl Acad Sci U S A 107:17957-17961

Imai T, Sun S-j, Horikawa Y, Wada M, Sugiyama J (2014) Functional reconstitution of cellulose synthase in Escherichia coli. Biomacromolecules 15:4206-4213

Isogai A (2013) Wood nanocelluloses: fundamentals and applications as new bio-based nanomaterials. J Wood Sci 59: 449-459

Ito K, Akiyama Y (1991) *In vivo* analysis of integration of membrane proteins in *Escherichia coli*. Mol Microbiol 5:2243-2253

Itoh T, Kimura S, Brown Jr. RM (2007) Immunogold labeling of cellulosesynthesizing terminal complexes. In: Brown Jr. RM, Saxena IM (ed) Cellulose: Molecular and Structural Biology. Springer: Netherlands, pp237-255.

Iyer PR, Catchmark J, Brown NR, Tien M (2011) Biochemical localization of a protein involved in synthesis of *Gluconacetobacter hansenii* cellulose. Cellulose 18:739-747

Kawano S, Tajima K, Kono H, Erata T, Munekata M, Takai M (2002) Effects of endogenous endo-β-1,4-glucanase on cellulose biosynthesis in *Acetobacter xylinum* ATCC23769. Journal of Bioscience and Bioengineering 94:275-281

Kawano S, Tajima K, Kono H, Numata Y, Yamashita H, Satoh Y, Munekata M (2008) Regulation of endoglucanase gene (cmcax) expression in *Acetobacter xylinum*. Journal of Bioscience and Bioengineering 106:88-94

Kawano S, Tajima K, Uemori Y, Yamashta H, Erata T, Munekata M, Takai M (2002) Cloning of cellulose synthesis related genes from *Acetobacter xylinum* ATCC23769 and ATCC53582: comparison of cellulose synthetic ability between strains. DNA Res 9:149-156

Keiski C-L, Harwich M, Jain S, Neculai AM, Yip P, et al. (2010) AlgK is a TPR-containing protein and the periplasmic component of a novel exopolysaccharide secretin. Structure.18: 265-73.

Kimura S, Chen HP, Saxena IM, Brown Jr. RM, Itoh T (2001) Localization of cdi-GMP-binding protein with the linear terminal complexes of *Acetobacter xylinum*. J Bacteriol 183:5668-5674

Kimura S, Laosinchai W, Itoh T, Cui X, Linder CR, Brown Jr. MR (1999) Immunogold labeling of rosette terminal cellulose-synthesizing complexes in the vascular plant Vigna angularis. Plant Cell 11:2075-2085

Klemm D, Schumann D, Kramer F (2009) Nanocellulose Materials-different cellulose, different functionality. Macromolecular Symposia 280: 60-70

Kobayashi S, Hobson LJ, Sakamoto J, Kimura S, Sugiyama J, Imai T, Itoh T (2000) Formation and structure of artificial cellulose spherulites via enzymatic polymerization. Biomacromolecules 1:168-173

Kolpak FJ and Blackwell J (1976) Determination of the structure of cellulose II. Macromolecules 9:273-278

Komeili A, Li Z, Newman DK, Jensen GJ (2006) Magnetosomes are cell membrane imaginations organized by the actin-like protein MamK. Science 311:242-245

Koo HM, Song SH, Pyun YR, Kim YS (1998) Evidence That a β-1,4-endoglucanase secreted by *Acetobacter xylinum* plays an essential role for the formation of cellulose fiber. Biosci Biotechnol Biochem 62:2257-2259

Koyama M, Helbert W, Imai T, Sugiyama J, Henrissat B (1997) Parallel-up structure evidences the molecular directionality during biosynthesis of bacterial cellulose. Proc Natl Acad Sci U S A 94:9091-9095

Kudlicka K, Brown Jr RM (1997) Cellulose and callose biosynthesis in higher plants. I. Solubilization and separation of (1,3)- and (1,4)-β-glucan synthase activities from mung bean. Plant Physiol 115:643-56

Kudlicka K, Brown R, Li L, Lee J, Shin H, Kuga S (1995) β-glucan synthesis in the cotton fiber. IV. In vitro assembly of the cellulose I allomorph. Plant Physiol. 107:111-23

Kuga S, Takagi S, Brown Jr. RM (1993) Native folded-chain cellulose II. Polymer 34:3293-3297

Lai-Kee-Him J, Chanzy H, Müller M, Putaux JL, Imi T, Bulone V (2002) In vitro versus in vivo cellulose microfibrils from plant primary wall synthases: Structural differences. J Biol Chem 277: 36931-36939

Langan P, Nishiyama Y, Chanzy H (2001) X-ray structure of mercerized cellulose II at 1 Å resolution. Biomacromolecules 2:410-416

Lei L, Zhang T, Strasser R, Lee CM, Gonneau M, Mach L, Vernhettes S, Kim SH, Cosgrove DJ, Li S, Gu Y (2014) The jiaoyao1 mutant is an allele of korrigan1 that abolishes endoglucanase activity and affects the organization of both cellulose microfibrils and microtubules in Arabidopsis. Plant Cell 26:2601-2616

Li S, Lei L, Somerville CR, Gu Y (2012) Cellulose synthase interactive protein 1 (CSI1) links microtubules and cellulose synthase complexes. Proc Natl Acad Sci USA 109:185-190

Lin FC, Brown Jr. RM (1988) Purification of cellulose synthase from *Acetobacter xylinum*. In: Schuerch C (ed) Cellulose and wood - Chemistry and Technology. John Wiley & Sons, Inc., New York, pp 473-492

Martinez-Morales F, Borges AC, Martinez A, Shanmugam KT, Ingram LO (1999) Chromosomal integration of heterologous DNA in Escherichia coli with precise removal of markers and replicons used during construction. J Bacteriol 181: 7143-7148

Mazur O and Zimmer J (2011) Apo- and Cellopentaose-bound Structures of the Bacterial Cellulose Synthase Subunit BcsZ. The Journal of Biological Chemistry 286: 17601-17606

McNamara JT, Morgan JLW, Zimmer J (2015) A molecular description of cellulose biosynthesis. Annual Review of Biochemistry 84:895-921

Mei Y, Gao HB, Yuan M, Xue HW (2012) The Arabidopsis ARCP protein, CSI1, which is required for microtubule stability, is necessary for root and anther development. Plant Cell 24:1066-1080

Meyer KH, Misch L (1937) Positions des atomes dans le nouveau modele spatiall **de** la cellulose. Helv Chim Acta 20:232-244

Mizrachi E, Mansfield SD, Myburg AA (2012) Cellulose factories: advancing bioenergy production from forest trees. New Phytologist 194: 54-62

Monteiro C, Saxena I, Wang X, Kader A, Bokranz W, Simm R, Nobles D, Chromek M, Brauner A, Brown Jr. RM, Römling U (2009) Characterization of cellulose production in Escherichia coli Nissle 1917 and its biological consequences. Environ Microbiol 11:1105-1116

Morgan JLW, McNamara JT, Fischer M, Rich J, Chen HM, Withers SG, Zimmer J (2016) Observing cellulose biosynthesis and membrane translocation in crystallo. Nature 531:329-334. doi: 10.1038/nature16966 [doi]

Morgan JLW, McNamara JT, Zimmer J (2014) Mechanism of activation of bacterial cellulose synthase by cyclic di-GMP. Nature Structural and Molecular Biology 21:489-496

Morgan JLW, Strumillo J, Zimmer J (2013) Crystallographic snapshot of cellulose synthesis and membrane translocation. Nature 493:181-186

Nagahashi S, Sudoh M, Ono N, Sawada R, Yamaguchi E, Uchida Y, Mio T, Takagi M, Arisawa M, Yamada-Okabe H (1995) Characterization of chitin synthase 2 of saccharomyces cerevisiae. Implication of two highly conserved domains as possible catalytic sites. J Biol Chem 270:13961-13967

Nakai T, Moriya A, Tonouchi N, Tsuchida T, Yoshinaga F, Horinouchi S, Sone Y, Mori H, Sakai F, Hayashi T (1998) Control of expression by the cellulose synthase (bcsA) promoter region from *Acetobacter xylinum* BPR 2001. Gene 213:93-100

Nakai T, Sugano Y, Shoda M, Sakakibara H, Oiwa K, Tuzi S, Imai T, Sugiyama J, Takeuchi M, Yamauchi D, Mineyukia Y (2013) Formation of highly twisted

ribbons in a carboxymethylcellulase gene-disrupted strain of a cellulose producing bacterium. J Bacteriol 195:958-964

Nicol F, His I, Jauneau A, Vernhettes S, Canut H, Hofte H (1998) A plasma membrane-bound putative endo-1,4-β-D-glucanase is required for normal wall assembly and cell elongation in Arabidopsis. EMBO J. 17:5563-76

Niimura H, Yokoyama T, Kimura S, Matsumoto Y, Kuga S (2010) AFM observation of ultrathin microfibrils in fruit tissues. Cellulose 17:13-18

Nishiyama Y, Langan P, Chanzy H (2002) Crystal structure and hydrogen-bonding system in cellulose Iβ from synchrotron X-ray and neutron fiber diffraction. J Am Chem Soc 124:9074-9082

Nishiyama Y, Sugiyama J, Chanzy H, Langan P (2003) Crystal Structure and Hydrogen Bonding System in Cellulose Iα from Synchrotron X-ray and Neutron Fiber Diffraction. J Am Chem Soc 125:14300-14306

Nobles DR, Brown Jr. RM (2008) Transgenic expression of *Gluconacetobacter xylinus* strain ATCC 53582 cellulose synthase genes in the cyanobacterium Synechococcus leopoliensis strain UTCC 100. Cellulose 15:691-701

Okano T, Sarko A (1985) Mercerization of cellulose, II. Alkali-cellulose intermediates and a possible mercerization mechanism. J Appl Polym Sci 30:325-332

Okuda K, Li L, Kudlicka K, Kuga S, Brown Jr. RM (1993) β-Glucan synthesis in the cotton fiber: I. Identification of β-1,4- and β-1,3-glucans synthesized in vitro. Plant Physiol 101:1131-1142

Omadjela O, Narahari A, Strumillo J, Mélida H, Mazur O, Bulone V, Zimmer J (2013) BcsA and BcsB form the catalytically active core of bacterial cellulose synthase sufficient for in vitro cellulose synthesis. Proc Natl Acad Sci U S A 110:17856-17861

Paredez A, Somerville CR, Ehrhardt D (2006) Dynamic visualization of cellulose synthase demonstrates functional association with cortical microtubules. Science 312:1491-95

Paredez AR, Persson S, Ehrhardt DW, Somerville CR (2008) Genetic evidence that cellulose synthase activity influences microtubule cortical array organization. Plant Physiol 147:1723-1734

Payen A. (1838) Mémoire sur la composition du tissu propre des plantes et du ligneux. C R Hebd Séances Acad Sci 7:1062-1056

Pear JR, Kawagoe Y, Schreckengost WE, Delmer DP, Stalke DM (1996) Higher plants contain homologs of the bacterial celA genes encoding the catalytic subunit of cellulose synthase. Proc Natl Acad Sci U S A 93 (22): 12637-12642

Peng L, Kawagoe Y, Hogan P, Delmer D (2002) Sitosterol-β-glucoside as primer for cellulose synthesis in plants. Science 295:147-150

Pérez S and Mackie B 2001 in https://www.cermav.cnrs.fr/lessons/cellulose/contenu/Chap_8/index_8.html

Preston RD (1974). The physical biology of plant cell walls. London.: Chapman & Hall.

Purushotham P, Cho SH, Díaz-Moreno SM, Kumar M, Nixon BT, Bulone V, Zimmer J (2016) A single heterologously expressed plant cellulose synthase isoform is sufficient for cellulose microfibril formation in vitro. Proc Natl Acad Sci U S A 113:11360-11365

Rao F, Pasunooti S, Ng Y, Zhuo W, Lim L, Liu AW, Liang Z (2009) Enzymatic synthesis of c-di-GMP using a thermophilic diguanylate cyclase. Anal Biochem 389:138-142

Richmond T (2000) Higher plant cellulose synthases. Genome Biol 4:30011-30016

Robert S, Bichet A, Grandjean O, Kierzkowski D, Satiat-Jeunemaitre B, Hauser MT, Höftea H, Vernhettes S (2005) An Arabidopsis endo-1,4-β-D-glucanase involved in cellulose synthesis undergoes regulated intracellular cycling. Plant Cell 17:3378-3389

Römling U, Galperin MY (2015) Bacterial cellulose biosynthesis: Diversity of operons, subunits, products, and functions. Trends Microbiol 23:545-557

Ross P, Mayer R, Weinhouse H, Amikam D, Huggirat Y, Benziman M, De Vroom E, Fidder A, De Paus P, Sliedregt LAJM, Van Der Marel GA, Van Boom JH (1990) The cyclic diguanylic acid regulatory system of cellulose synthesis in *Acetobacter xylinum*. Chemical synthesis and biological activity of cyclic nucleotide dimer, trimer, and phosphothioate derivatives. J Biol Chem 265:18933-18943

Ross P, Weinhouse H, Aloni Y (1987) Regulation of cellulose synthesis in *Acetobacter xylinum* by cyclic diguanylic acid. Nature 325:279-281

Salonen LM, Ellermann M, Diederich F (2011) Aromatic rings in chemical and biological recognition: Energetics and structures. Ang Chem Internat Ed 50: 4808-4842

Maleki SS, Mohammadi K, Ji K, (2016) Characterization of Cellulose Synthesis in Plant Cells. The Scientific World Journal 2016 ID:8641373

Sarko A (1978) What is the crystalline structure of cellulose? TAPPI 61:59-61

Sarko A and Muggli R (1974) Packing analysis of carbohydrates and polysaccharides. III. Valonia cellulose and cellulose II. Macromolecules 7:486-494

Sato S, Kato T, Kakegawa K, Ishii T, Liu YG, Awano T, Takabe K, Nishiyama Y, Kuga S, Sato S, Nakamura Y, Tabata S, Shibata D (2001) Role of the putative membrane-bound endo-1,4-β-glucanase KORRIGAN in cell elongation and cellulose synthesis in Arabidopsis thaliana. Plant Cell Physiol. 42:251-63

Saxena IM, Brown Jr. RM (1997) Identification of cellulose synthase(s) in higher plants: Sequence analysis of processive -glycosyltransferases with the common motif 'D, D, D35Q(R, Q) XRW'. Cellulose 4:33-49

Saxena IM, Brown Jr. RM (2012) Biosynthesis of bacterial cellulose. In M gama, P Gatenbolm, D Kemm (ed) Bacterial nanocellulose: a sophisticatd multifunctional material, FL: CRC Boca Ration, pp.1-18

Saxena IM, Brown Jr. RM, Fevre M, Geremia RA, Henrissat B (1995) Multidomain architecture of β-glycosyl transferases: Implications for mechanism of action. J Bacteriol 177:1419-1424

Saxena IM, Kudlicka K, Okuda K, Brown Jr. RM (1994) Characterization of genes in the cellulose-synthesizing operon (acs operon) of *Acetobacter xylinum*: Implications for cellulose crystallization. J Bacteriol 176:5735-5752

Saxena IM, Lin FC, Brown Jr RM (1990) Cloning and sequencing of the cellulose synthase catalytic subunit gene of *Acetobacter xylinum*. Plant Mol Biol 15: 673-683

Scheffel A, Gruska M, Faivre D, Linaroudis A, Plitzko JM, Schu¨ler1 D (2006) An acidic protein aligns magnetosomes along a filamentous structure in magnetotactic bacteria. Nature 440: 110-114

Schramm M, Hestrin S (1954) Factors affecting production of cellulose at the air/liquid interface of a culture of *Acetobacter xylinum*. J Gen Microbiol 11:123-129

Serra DO, Richter AM, Hengge R (2013) Cellulose as an architectural element in spatially structured *Escherichia coli* biofilms. J Bacteriol 195:5540-5554

Sethaphong L, Haigler CH, Kubicki JD, Zimmer J, Bonetta D, DeBolt S, Yingling YG (2013) Tertiary model of a plant cellulose synthase. Proc Natl Acad Sci U S A 110: 7512-7517

Shibazaki H, Kuga S, Onabe F, Brown Jr. RM (1995) Acid hydrolysis behaviour of microbial cellulose II. Polymer 36:4971-4976

Simon I, Glasser L, Scheraga H A and Manley RSt J (1988b) Structure of cellulose. 2. Low- energy crystalline arrangements. ibid. 21:990-998

Slabaugh E, Davis JK, Haigler CH, Yingling YG, Zimmer J (2014) Cellulose synthases: New insights from crystallography and modeling. Trends Plant Sci 19:99-106

Somerville C (2006) Cellulose synthesis in higher plants. Annual Review of Cell and Developmental Biology 22:53-78

Stahlberg J, Johansson G, Pettersson G (1993) Trichoderma reesei has no true exo-cellulase: all intact and truncated cellulases produce new reducing end groups on cellulose. Biochim. Biophys Acta 1157:107-113

Standal R, Iversen T-G, Coucheron DH, Fjaervik E, Blatny JM, Valla S (1994) A new gene required for cellulose production and a gene encoding cellulolytic activity in *Acetobacter xylinum* are colocalized with the bcs operon. J Bacteriol 176:665-672

Stipanovic AJ and Sarko A (1976) Packing analysis of carbohydrates and polysaccharides. 6. Molecular and crystal structure of regenerated cellulose II. Macromolecules 9:851-857

Su H-, Lee T-, Huang Y-, Chou S-, Wang J-, Lin L-, Chow T- (2011) Increased cellulose production by heterologous expression of cellulose synthase genes in a filamentous heterocystous cyanobacterium with a modification in photosynthesis performance and growth ability. Botanical Studies 52:265-275

Sugiyama J, Persson J, Chanzy H (1991a) Combined infrared and electron diffraction study of the polymorphism of native celluloses. Macromolecules 24:2461-2466

Sugiyama J, Vuong R, Chanzy H (1991b) Electron diffraction study on the two crystalline phases occurring in native cellulose from an algal cell wall. Macromolecules 24:4168-4175

Sun S-j, Horikawa Y, Wada M, Sugiyama J, Imai T (2016) Site-directed mutagenesis of bacterial cellulose synthase highlights sulfur-arene interaction as key to catalysis. Carbohydr Res 434:99-106

Sunagawa N, Fujiwara T, Yoda T, Kawano S, Satoh Y, Yao M, Tajima K, Dairi T (2013) Cellulose complementing factor (Ccp) is a new member of the cellulose synthase complex (terminal complex) in *Acetobacter xylinum*. Journal of Bioscience and Bioengineering 115:607-612

Szyjanowicz PMJ, McKinnon I, Taylor NG, Gardiner J, Jarvis MC, Turner SR (2004) The irregular xylem 2 mutant is an allele of korrigan that affects the secondary cell wall of Arabidopsis thaliana. Plant J. 37:730-40

Thormann KM, Duttler S, Saville RM, Hyodo M, Shukla S, Hayakawa Y, Spormann AM (2006) Control of formation and cellular detachment from Shewanella oneidensis MR-1 biofilms by cyclic di-GMP. J Bacteriol 188:2681-2691

Tonouchi N, Tahara N, Kojima Y, Nakai T, Sakai F, Hayashi T, Tsuchida T, Yoshinaga F (1997) Abeta-glucosidase gene downstream of the cellulose synthase operon in cellulose-producing *Acetobacter*. Biosci Biotechnol Biochem. 61:1789-1790

Updegraff DM (1969) Semimicro determination of cellulose inbiological materials. Anal Biochem 32:420-424

Vain T, Crowell EF, Timpano H, Biot E, Desprez T, Mansoori N, Trindade LM, Pagant S, Robert S, Höfte H, Gonneau M, Vernhettes S (2014) The cellulase KORRIGAN is part of the cellulose synthase complex. Plant Physiol 165:1521-1532

VanderHart DL, Atalla R H (1984) Studies of microstructure in native celluloses using solid-state carbon-13 NMR. Macromolecules 17: 1465-1472

Wada M, Okano T, Sugiyama J (2001) Allomorphs of native crystalline cellulose I evaluated by two equatorial d-spacings. Journal of Wood Science 47:124-128

Wertz JL, Bédué O, Mercier JP (2010) Cellulose Science and Technology. In: Wertz JL (ed) Structure and properties of cellulose.EPFL Press Italy, pp 90

Wong HC, Fear AL, Calhoon RD, Eichinger GH, Mayer R, Amikam D, Benziman M, Gelfand DH, Meade JH, Emerick AW, Bruner R, Ben-Bassat A, Tal R (1990) Genetic organization of the cellulose synthase operon in *Acetobacter xylinum*. Proc Natl Acad Sci U S A 87:8130-8134

Yamamoto H, Horii F, Odani H (1989) Structural changes of native cellulose crystals induced by annealing in aqueous alkaline and acidic solutions at high temperatures. Macromolecules 22:4130-4132

Yano H (2012) Production of cellulose nanofibres and their applications. Nippon Gomu Kyokaishi 12:376-381

Zeytuni N, Zarivach R (2012) Structural and Functional Discussion of the Tetra-Trico-Peptide Repeat, a Protein Interaction Module. Structure 20:397-405

Zogaj X, Nimtz M, Rohde M, Bokranz W, Römling U (2001) The multicellular morphotypes of *Salmonella typhimurium* and *Escherichia coli* produce cellulose as the second component of the extracellular matrix. Mol Microbiol 39*:* 1452-1463

Zuo JR, Niu QW, Nishizawa N,Wu Y, Kost B, Chua NH (2000) KORRIGAN, an Arabidopsis endo-1,4-β-glucanase, localizes to the cell plate by polarized targeting and is essential for cytokinesis. Plant Cell 12:1137-52

Acknowledgements

This thesis could not be completed without the help of many people.

My deepest gratitude goes first to my supervisor Professor Junji Sugiyama. He guided me to know the direction of the research, encouraged and gave me a lot of advices. Also when I have a baby, gave me a lot of priority for taking care of my baby.

I also must be deeply grateful to Associate Professor Tomoya Imai, he guided me a lot on research and experiments, which was indeed essential to complete this thesis. Each time when I have a question, he is kindly reply. In addition, the earnest work manner from him is very worth me to learn.

I would like to thank Professor Keiji Takabe and Professor Toshiaki Umezawa for critical reading and suggestion valuable comments on examining my thesis.

I also want to thank Associate Professors Satoshi Kimura in the Graduate School of Agricultural and Life Science, Tokyo University, Masahisa Wada in the Graduate School of Agriculture, Kyoto University and Yoshiki Horikawa in Faculty of Agriculture, Tokyo University of Agriculture and Technology gave me a lot supports on my papers.

My appreciation also extended to all the Professors in RISH of Kyoto University.

I would like to thank Assistant Professor Kei'ichi Baba and Suyako Tazuru kindly gave me advices and information whatever in the research or life.

I also owe my sincere gratitude to the entire member in Lab. Biomass Morphogenesis and friends in other Labs. You give me a lot of pleasant memories in Kyoto, Japan.

At last, I would like say thanks to my family. If without helps and encouragement from you, I cannot go well on doctor course period. Finally, I am deeply indebted to Mr. Zhongyuan Zhao for his continuing support and encouragement.